



2022

# MICROBIAL COMMUNITY ANALYSIS: BIOFILM INHIBITION & ALGAE ASSOCIATED COMMUNITY STRUCTURE

Michelle V. Fong  
*University of the Pacific*

Follow this and additional works at: [https://scholarlycommons.pacific.edu/uop\\_etds](https://scholarlycommons.pacific.edu/uop_etds)



Part of the [Ecology and Evolutionary Biology Commons](#), [Microbiology Commons](#), and the [Molecular Biology Commons](#)

## Recommended Citation

Fong, Michelle V.. (2022). *MICROBIAL COMMUNITY ANALYSIS: BIOFILM INHIBITION & ALGAE ASSOCIATED COMMUNITY STRUCTURE*. University of the Pacific, Thesis.  
[https://scholarlycommons.pacific.edu/uop\\_etds/3824](https://scholarlycommons.pacific.edu/uop_etds/3824)

This Thesis is brought to you for free and open access by the University Libraries at Scholarly Commons. It has been accepted for inclusion in University of the Pacific Theses and Dissertations by an authorized administrator of Scholarly Commons. For more information, please contact [m gibney@pacific.edu](mailto:m gibney@pacific.edu).

MICROBIAL COMMUNITY ANALYSIS:  
BIOFILM INHIBITION & ALGAE ASSOCIATED COMMUNITY STRUCTURE

By

Michelle Victoria Fong

A Thesis Submitted to the

Graduate School

In Partial Fulfillment of the

Requirements for the Degree of

MASTER OF SCIENCE

Thomas J. Long School of Pharmacy  
Pharmaceutical and Chemical Sciences

University of the Pacific  
Stockton, CA

2022

MICROBIAL COMMUNITY ANALYSIS:  
BIOFILM INHIBITION & ALGAE ASSOCIATED COMMUNITY STRUCTURE

By

Michelle Victoria Fong

APPROVED BY:

Thesis Advisor: Skylar Carlson, Ph.D.

Committee Member: Jerry Tsai, Ph.D.

Committee Member: Joseph Harrison, Ph.D.

Committee Member: Paul Orwin, Ph.D.

Department Co-Chair: Jianhua Ren, Ph.D.

Department Co-Chair: Jerry Tsai, Ph.D.

**MICROBIAL COMMUNITY ANALYSIS:  
BIOFILM INHIBITION & ALGAE ASSOCIATED COMMUNITY STRUCTURE**

Copyright 2022

By

Michelle Victoria Fong

## DEDICATION

This thesis is dedicated to my parents, Stanley and Victoria Fong. Thank you for constantly supporting and believing in me.

## ACKNOWLEDGEMENTS

First, I would like to send my gratitude to Dr. Skylar Carlson for allowing me to start in her lab in the middle of COVID and for her guidance throughout my time here. I am grateful for the opportunities she has given me and for pushing me to become a better scientist.

I would like to thank my thesis committee, Dr. Jerry Tsai, Dr. Joseph Harrison and Dr. Paul Orwin. Thank you to Dr. Tsai for seeing potential in me and encouraging me to join the chemistry graduate program. Thank you to Dr. Harrison for sparking my interest in research as an undergrad in your lab and for being a mentor to me throughout my time at UOP. Thank you to Dr. Orwin for joining my committee last minute and allowing me to work on your project.

These projects would have not been possible without the help of many people. For the biofilm project, I would like to thank Esther Gomez for providing me with the filtered media, Dr. Orwin for his guidance on antiSMASH and the biofilm inhibition assay, and Dr. Laura Sanchez and her research group at University of California, Santa Cruz for running LC-MS/MS on my extracts using their instruments. For the Caulerpa ID project, I would like to thank Dr. Melany Puglisi-Weening and her research group from Chicago State University for providing me with the bacterial isolates, Dr. Harrison for allowing me to use his PCR reagents and thermal cycler, Dr. Orwin for his help in PCR troubleshooting, Carolyn Keim for training me at the beginning of this project, and my undergrads Lynn Sasaki and Katy Kim for their help running PCR and PCR gels. For the microalgae project, I would like to thank Dr. Carolyn Fisher and Dr. Todd Lane from Lawrence Livermore National Laboratory for allowing me to write the manuscript using their data. The microalgae study has been submitted as a short communications paper to Algal Research titled “Cryo-storage and algal association of protective

bacteria that protect *Microchloropsis salina* from grazing by *Brachionus plicatilis*” on July 28, 2022.

I would like to express my gratitude to my lab mates in the Carlson lab – Carolyn Keim, Savannah Pierce, and Kara Talbott. I’m grateful for your support both in and outside of the lab. I would like to thank the undergraduate researchers in the Carlson lab for their help.

Lastly, I would like to thank my family for their never-ending support throughout my time here at UOP. I wouldn’t be the person I am today without you all.

## MICROBIAL COMMUNITY ANALYSIS: BIOFILM INHIBITION & ALGAE ASSOCIATED COMMUNITY STRUCTURE

### Abstract

By Michelle Victoria Fong

University of the Pacific  
2022

Natural products chemistry is the pursuit of bioactive small molecules from living organisms. These can be classified as primary metabolites if they are essential to survival, and secondary metabolites if they are accessory, playing a role in communication, defense, recruitment, etc.. Natural products have made a significant contribution to society – of 1,881 FDA-approved drugs from 1981 to 2019, 4% were pure natural products, 19% were natural products derived, and 3% were synthetic drugs with a natural products pharmacophore targeting a wide range of diseases and infections (Newman & Cragg, 2020). Pharmacophores are structural components of drugs that are responsible for the observed biological activity. Natural products often contain unique pharmacophores that exhibit potent bioactivity, thereby serving as inspiration for synthetic chemists to manufacture exciting new drug leads.

Bacteria are ubiquitous in the environment. Marine bacteria are a prolific source of chemically diverse natural products due to the high biodiversity and competition in the marine environment. In 2018, 240 new marine natural products were reported in the literature from bacteria (Carroll et al., 2020). It is hypothesized that secondary metabolites offer an advantage to the producer, however, the roles that natural products play in their environment are not as well characterized. These pursuits are classified as chemical ecology. Throughout my thesis, I aim to



identify the bacteria present from these environments and begin to understand the ecological role small molecules play in their environment.

*Staphylococcus aureus* is notorious for causing chronic infections and resisting therapeutic treatment by forming biofilms. Biofilms are extracellular polymeric substance (EPS) matrices containing bacteria that attach to biotic and abiotic surfaces. The EPS matrix provides a refuge and anchorage to a surface, allowing biofilm inhabitants to be shielded from full strength of therapeutic treatments leading to resistance. *Variovorax paradoxus* is a gram-negative bacteria that also produces biofilms. It has been previously reported that *V. paradoxus* inhibits *S. aureus* biofilm formation. Preliminary data suggests *V. paradoxus* produces a small molecule that has biofilm inhibition activity. My work focuses on characterizing a GLP and another secondary metabolite produced by *V. paradoxus* that inhibits *S. aureus* biofilms through both molecular biology and natural products chemistry.

*Caulerpa* spp. is a macroalgae native to tropical and subtropical oceans. Due to global warming, the temperature of oceans continues to rise, allowing *Caulerpa* spp. to inhabit higher latitudes. It has been hypothesized that successful invasion occurs by outcompeting native organisms via exerting adverse effects on the surrounding environment. The secondary metabolites of this algae are well characterized however their ecological role is hardly characterized. We hypothesize that *Caulerpa* spp. could be chemically mediating its surface microbiome by recruiting a higher percentage of *Vibrio* spp.. *Vibrio* spp. are known pathogens to humans and marine organisms by causing infections and forming biofilms. My goal was to identify a panel of culturable *Caulerpa* spp. surface-associated bacteria through molecular and microbiology methods.

Microalgae are an exciting alternative source of biofuels. However, microalgae are grown in open algal ponds which are susceptible to crashing causing the total loss of an algal crop. Pond crashes are caused by a number of factors, one of which is contamination by unwanted pests such as protozoans and fungi. Previous studies focused on the use of bacterial communities as a built-in biocontrol to inhibit pests from causing algal pond crashes. Preliminary data demonstrated the addition of a bacterial community protected the microalgae *Microchloropsis salina* from grazing by the marine rotifer *Brachionus plicatilis* (Fisher et al., 2019). My work focuses on analyzing the composition of the protective bacterial community added to the microalgae that have been size filtered to observe bacterial association with algae, rotifers, or free-floating. *M. salina* cultures in the presence and absence of *B. plicatilis* were analyzed for the identification of protective bacterial species that were algae-, rotifer-associated, or free-floating. This work has been submitted to the journal Algal Research and is under review (Fisher et al., 2022).

Bacteria play a significant role in their environment. The identification of bacterial species and the role their suite of small molecules play is crucial to fully characterizing the observed interactions. My thesis surveys several means of bacterial community analysis through identification and small molecule characterization.

## TABLE OF CONTENTS

List of Tables.....	13
List of Figures.....	14
List of Abbreviations.....	15
Chapter 1: Introduction.....	19
1.1 Natural Products Chemistry.....	19
1.2 Marine Bacteria as a Natural Products Source.....	20
1.3 Role of Natural Products in Bacterial Communication.....	21
Chapter 2: Characterization of a Small Molecule Produced by <i>Variovorax paradoxus</i> EPS.....	24
2.1 Background.....	24
2.1.1 Biofilms.....	24
2.1.2 <i>Variovorax paradoxus</i> .....	26
2.1.3 Glycolipopeptides (GLPs).....	27
2.1.4 Natural Products Workflow.....	28
2.1.5 Genome Mining.....	30
2.2 Materials and Methods.....	32
2.2.1 Bacterial Strains and Culture Conditions.....	32
2.2.2 Extraction and Fractionation.....	32
2.2.3 LC-MS/MS Data Analysis.....	35
2.2.4 Biofilm Inhibition Assay.....	35
2.3 Results and Discussion.....	36
2.3.1 Extraction and LC-MS/MS on Crude Extracts.....	36

	11
2.3.2 GLP Production by <i>V. paradoxus</i> .....	40
2.3.3 Fractionation and Biofilm Inhibition Assay.....	42
2.3.4 Genome Mining using antiSMASH.....	43
2.4 Summary.....	47
Chapter 3: Identification of Culturable <i>Caulerpa</i> spp. Surface-Associated Bacteria.....	48
3.1 Background.....	48
3.1.1 <i>Caulerpa</i> spp.....	48
3.1.2 <i>Vibrio</i> spp. and Vibriosis.....	50
3.1.3 Bacterial Identification.....	51
3.1.4 Agar Typing of Marine Bacteria.....	53
3.2 Materials and Methods.....	54
3.2.1 Bacterial Isolation.....	54
3.2.2 DNA Extraction.....	54
3.2.3 PCR.....	55
3.2.4 Sequencing and Identification.....	56
3.2.5 Agar Recipe.....	57
3.3 Results and Discussion.....	57
3.3.1 Identified Bacterial Strains.....	57
3.3.2 PCR Troubleshooting.....	58
3.3.3 Sequencing and Identification.....	63
3.3.4 Identification of <i>Vibrio</i> spp.....	64
3.4 Summary.....	69
Chapter 4: Protective Bacterial Community Associated with <i>Microchloropsis salina</i> .....	70

	12
4.1 Background.....	70
4.2 Summary.....	74
Chapter 5: Summary and Future Directions.....	75
References.....	76

## LIST OF TABLES

## Table

1. MIBiG Hits of Varpa 4519.....	46
2. PCR Primers to Target Specific Genes.....	56
3. Progress of Identification of 35 Isolated Bacterial Strains from the Surface of <i>Caulerpa</i> spp.....	62
4. Growth of <i>Vibrio</i> spp. on TCBS and MC Agar.....	67

## LIST OF FIGURES

## Figure

1. Structures of dalbavancin and telavancin.....	28
2. Fractionation trees of crude extracts of the two mono-cultures and two co-cultures.....	34
3. Mass spectra comparison of crude extracts.....	38
4. MS/MS spectra of VP EPS and V+S crude extracts.....	39
5. Structure of NB-RLP1006, a GLP from <i>V. paradoxus</i> RKNM-096.....	41
6. Amino acid sequence alignment of <i>V. paradoxus</i> EPS and <i>V. paradoxus</i> RKNM-096.....	42
7. antiSMASH of <i>V. paradoxus</i> EPS.....	45
8. antiSMASH results of eighth BGC cluster from <i>V. paradoxus</i> EPS.....	45
9. Known abundant secondary metabolites produced by <i>Caulerpa</i> spp.....	49
10. 16S rRNA gene.....	52
11. Phylogenetic tree of identified bacterial strains.....	58
12. PCR gel for the amplification of the 16S rRNA gene.....	59
13. Genomic DNA gel.....	60
14. Sequencing results of the 16S rRNA gene.....	64
15. Agar plates to identify <i>Vibrio</i> spp. based on morphology.....	66
16. PCR gel for the amplification of the <i>toxR</i> gene.....	68
17. PCR gel for the amplification of the <i>hsp60</i> gene.....	69

## LIST OF ABBREVIATIONS

35+S	<i>V. paradoxus</i> mutant strain 35 and <i>S. aureus</i> co-culture
A	adenylation domain
antiSMASH	antibiotics and Secondary Metabolite Analysis Shell
BGC	biosynthetic gene cluster
BLAST	Basic Local Alignment Search Tool
bp	base pairs
°C	degree Celsius
C	condensation domain
CHCl <sub>3</sub>	chloroform
Da	daltons
ddNTPs	dideoxynucleotide triphosphates
DI	deionized
DMSO	dimethyl sulfoxide
DNA	deoxyribonucleic acid
dNTPs	deoxyribonucleotide triphosphates
EPS	extracellular polymeric substance
EtOAc	ethyl acetate
E-value	Expect value
FDA	U.S. Food and Drug Administration
g	gram
g/L	gram per liter



GLP	glycolipopeptide
h	hour
HPLC	high-performance liquid chromatography
ISP2	International <i>Streptomyces</i> Project-2
kb	kilobase
L	liter
LC/MS	liquid chromatography mass spectrometry
LC-MS/MS	liquid chromatography tandem mass spectrometry
$m/z$	mass-to-charge ratio
MC	MacConkey
MeOH	methanol
mg	milligram
mg/L	milligram per liter
mg/mL	milligram per milliliter
MIBiG	Minimum Information about a Biosynthetic Gene Cluster
mL	milliliter
MS	mass spectrometry
MS/MS	tandem mass spectrometry
MW	molecular weight
NCBI	National Center for Biotechnology Information
ng/ $\mu$ L	nanogram per microliter
nm	nanometer
NMR	nuclear magnetic resonance

NRPS	non-ribosomal peptide synthetase
OD <sub>595</sub>	optical density at 595 nm
OTU	operational taxonomic unit
PCP	peptidyl carrier protein domain
PCR	polymerase chain reaction
PKS	polyketide synthetase
pmol/μL	picomole per microliter
ret	retentate
RPM	rotations per minute
rRNA	ribosomal ribonucleic acid
sp.	singular species
SPE	solid phase extraction
spp.	several species
TCBS	Thiosulfate-Citrate-Bile Salts-Sucrose
TD	terminal reductase domain
TIC	total ion chromatogram
μg/mL	microgram per milliliter
μL	microliter
μm	micrometer
UHPLC	ultra high performance liquid chromatography
V+S	<i>V. paradoxus</i> strain EPS and <i>S. aureus</i> co-culture
VP EPS	<i>Variovorax paradoxus</i> strain EPS
VP Mut 35	<i>V. paradoxus</i> mutant strain 35

xg	relative centrifugal force
XIC	extracted ion chromatogram
YE	yeast extract

## CHAPTER 1: INTRODUCTION

### 1.1 Natural Products Chemistry

Natural products chemistry is the pursuit of biologically active small molecules that are found from natural sources. Natural products are classified as primary metabolites if they are essential for growth and reproduction, and as secondary metabolites if they are not necessary for survival but play a role in communication, defense, recruitment, etc.. Secondary metabolites often display unique pharmacophores, contain multiple stereocenters, and are often complex structures (Harvey et al., 2015). Pharmacophores are structural features in a compound that are often responsible for the observed biological activity. Natural products studies have been historically focused terrestrial organisms, particularly plants, due to easy accessibility and human use as herbal remedies (Romano et al., 2017). Natural products derived from the marine environment are somewhat less developed due to accessibility and to the presumption that the marine environment contained the same chemistry as the terrestrial environment (Penesyan et al., 2010). With the introduction of scuba diving and techniques in the 1970s, there was a rapid improvement and explosion of studies from the marine environment (Dias et al., 2012).

A classic example of natural products in drug discovery is penicillin. Penicillin was discovered by Alexander Fleming in 1928 when he observed *Penicillium rubens* mold growing on an agar plate that inhibited bacterial growth. He extracted the mold and named the active component penicillin but was unable to isolate and purify the compound (Fleming, 1980). It was not until 1939 that Howard Florey and his colleagues successfully purified penicillin (Gaynes, 2017). In 1945, the structure of penicillin was established via X-ray crystallography by Dorothy Hodgkin at Oxford University (“Discovery and Development of Penicillin,” n.d.). Natural

products have made a significant contribution to human health. From 1981 to 2019 1,881 drugs have been FDA-approved targeting a wide range of diseases and infections in which 4% were pure natural products, 19% were natural products derived, and 3% were synthetic drugs with a natural products pharmacophore (Newman & Cragg 2020). The twentieth century was a turning point for the isolation and elucidation of natural products in regard to techniques and new sources (e.g., marine environment, bacteria, etc.). The advancement of computers and subsequently automated instrumentation has caused natural products chemistry to also advance (Xu et al., 2011). Natural products provide useful lead compounds with unique structural diversity and potent bioactivity for drug discovery.

### **1.2 Marine Bacteria as a Natural Products Source**

In 2018, bacterial sources accounted for 240 of new marine natural products reported in the literature (Carroll et al., 2020). Despite continuous discoveries, marine organisms and sediment remain a prolific source for novel natural products (Jain & Tailor, 2020). The implementation of scuba diving techniques allowed scientists to discover new source organisms, the compounds they produce, and to understand the interactions between organisms and the environment (Russo et al., 2011; Pawlik et al., 2013). Historically, there has been a focus on macro-organisms, such as algae, sponges, ascidians, tunicates and bryozoans (Dias et al., 2012). Macro-organisms are physically bigger and visually eye-catching, garnering attention to natural products scientists to study their metabolites. Natural products from macro-organisms are typically present at very low concentrations, requiring large biomass. For example, *Lissodendoryx* sp. is a rare, deep water sponge that produces halichondrin B, a macrolide with anticancer properties (Munro et al., 1999; Hirata & Uemura, 1986). Halichondrin B could not be distributed commercially through collections of the marine sponge. Various trials to transplant

the marine sponge to laboratories to grow and extract halichondrin B were successful at small scales, but for clinical trials an annual production of at least 5,000 tons of the marine sponge were necessary which is not practical (Munro et al., 1999).

Compared to macro-organisms, bacteria offer the alternative that they can be cultured in the laboratory at a large scale, thus increasing the amount of a natural product that can be obtained from one organism. For instance, actinomycetes are bacteria that have been reported to dedicate two-thirds of their genome to secondary metabolite biosynthesis (Udwary et al., 2007). Actinomycetes have produced various antibiotics that are still in use today (e.g., streptomycin, erythromycin, neomycin, and tetracyclines) (De Simeis & Serra, 2021). Due to the high biodiversity and competition in marine environments, the isolated bacteria often produce novel bioactive natural products that are not commonly seen in terrestrial bacteria (Jain & Tailor, 2020).

While natural products are widely identified for the purpose of drug discovery, their original function within their ecosystem are often not as well known (Schmidt et al., 2019). Many natural products are isolated based on their activity for therapeutic purposes and their ecological role is rarely considered. Environmental pressures have caused bacteria to produce chemically diverse natural products with bioactivity that are useful for drug discovery.

### **1.3 Role of Natural Products in Bacterial Communication**

There are many theories and hypotheses of the ecological roles natural products play in their environment, such as quorum sensing, competition or defense, attraction of other organisms, and synchronized specialized metabolism with other organisms (Daniel-Ivad et al., 2018; Petersen et al., 2020). Natural products can play a role as signaling molecules for communication between organisms. These secondary metabolites can be used in inter- or intra-

species communication (Daniel-Ivad et al., 2018). The identification of the specific role(s) natural products play in their environment is often overlooked in drug discovery efforts.

Bacteria often coexist in symbiotic relationships. Marine macro-organisms recruit and maintain their bacterial community on its surface or immediate surroundings through signaling molecules. Bacteria in turn produce small molecules for defense or may serve to scavenge metabolites for the host. The high specificity of bacterial communities associated with marine organisms emphasizes this close, chemically driven relationship (Penesyan et al., 2010). Often, marine macro-organisms produce compounds that act as chemical cues for the recruitment of bacteria to its surface or in close proximity to its benefit (Hay, 2009; Puglisi et al., 2014). This close relationship may give both organisms an advantage for survival. For example, the cyanobacteria *Trichodesmium* forms blooms (overgrowths) in nutrient-deficient oceans and it is hypothesized that this is due to the bacterial community it recruits for primary metabolites (Capone et al., 1997; M. Lee et al., 2017). Due to the dependency on the bacterial community for primary metabolites, the genome of *Trichodesmium* is hypothesized to be reduced based on the Black Queen Hypothesis (M. Lee et al., 2017). The Black Queen Hypothesis explains that if the production of a metabolite energetically costs too much to the host organism, it will recruit bacteria for production, and in turn the host organism loses the gene that was used to produce the metabolite (Morris et al., 2012). This is an ongoing project I worked on to identify the bacteria based on the 16S rRNA gene and primary metabolites produced by these bacteria to survive.

My thesis attempts to understand microbial interactions by identifying and analyzing bacterial communities and the natural products chemistry involved. In chapter 2, the characterization of a small molecule produced by *V. paradoxus* EPS was done through LC-MS/MS. Fractions of *V. paradoxus* EPS are being tested for their *S. aureus* biofilm inhibition

activity to identify the bioactive molecule. Surface-associated bacteria from the macroalgae *Caulerpa* spp. were identified to characterize the community that may be affected by chemical mediation in chapter 3. Protective bacterial communities added to ponds of the microalgae *M. salina* were analyzed according to their size association in chapter 4 to identify specific genera that protect *M. salina* from grazing by rotifers. Understanding the role a natural product plays in its environment is critical to understanding environmental pressures that could lead to ecological based drug discovery.



## CHAPTER 2: CHARACTERIZATION OF A SMALL MOLECULE PRODUCED BY

*VARIOVORAX PARADOXUS* EPS**2.1 Background****2.1.1 Biofilms**

The aim of this study is to characterize a GLP that has a molecular weight (MW) of 1,007 Da produced by a *V. paradoxus* strain and a second compound that was previously shown to inhibit *S. aureus* biofilm formation when grown together in co-culture (Gomez, 2022). The goal of this project is to characterize this second compound with biofilm inhibition activity via natural products chemistry and genome mining.

Biofilms are composed of bacteria encased by extracellular polymeric substance (EPS) matrices that attach to surfaces. Biofilms can either consist of a single or multiple microbial species, with the ability to adhere to a variety of biotic and abiotic surfaces (O'Toole et al., 2000). EPS matrices are composed of proteins, glycoproteins, glycolipids, and extracellular DNA (Flemming et al., 2007). Microbes in biofilms are protected from the host defense and antimicrobial compounds because the EPS matrix is resistant to phagocytes and diminishes antibiotic exposure, thereby delivering sublethal antibiotic doses leading to resistant microbes to survive and flourish (Otto, 2018). The development of biofilms is believed to occur in stages: 1) initial attachment to a surface, 2) colonization, 3) maturation of the biofilm, and 4) dispersion of cells (Tolker-Nielsen, 2015; Sharma et al., 2019).

Biofilms have been described as a fortress because biofilms enable microorganisms to survive in hostile environments such as starvation and desiccation, allowing them to persist and continue to cause diseases (Roy et al., 2018). Biofilm infections are a major cause of repeated

nosocomial infections, it has been estimated that biofilm cells can be up to 10,000 times more resistant to antibiotics than planktonic cells (Davies, 2003; Rabin et al., 2015). Biofilm-related infections respond to treatment in the beginning but frequently relapse, which may be due to multi-organism biofilm formation (Del Pozo, 2018).

*Staphylococcus aureus* is a Gram-positive bacteria that is commonly found on the skin but is also an opportunistic pathogen with the ability to form robust biofilms (Schilcher & Horswill, 2020). *S. aureus* is notorious for causing chronic infections and resisting therapeutic treatment via biofilm formation on implanted medical devices (Moormeier & Bayles, 2017). Strains resistant to frontline treatments, such as methicillin resistant *S. aureus* and multi-drug resistant *S. aureus* infections, are of concern because of their resistance to known treatments.

Research to treat biofilm-related infections is an ongoing struggle because biofilms have exhibited resistance to many therapeutic treatments as previously discussed. Current strategies to inhibit biofilms aim at the various stages of biofilm formation. At the initial attachment stage, biochemical (antimicrobial agents), physicochemical (coated surfaces), and biological (probiotic bacteria) approaches are in development (Yang et al., 2012). At the colonization and maturation stage, several strategies disrupt the EPS matrix enzymatically and chemically exposing resident biofilm cells via anti-biofilm agents and phages (Yang et al., 2012). Small molecules that exhibit anti-biofilm activity against various bacteria have been isolated from natural sources and made synthetically may provide a new strategy to combat biofilms (Roy et al., 2018; Yan et al., 2020). For example, lytic antimicrobial peptides were found to have biofilm inhibition activity against several bacterial biofilms that were isolated from natural sources and synthetically made (Yan et al., 2020). *V. paradoxus* forms poor biofilms and can be used as a new source for a small molecule with biofilm inhibition activity.

### 2.1.2 *Variovorax paradoxus*

*Variovorax paradoxus* is an aerobic Gram-negative bacteria that is found commonly in soil that contains aliphatic polycarbonates, arsenite, heavy metal ions, trichloroethylene, polychlorinated biphenyls, and sulfolane (Satola et al., 2013). *V. paradoxus* belongs to a group called plant growth-promoting rhizobacteria that can degrade hazardous contaminants (Han et al., 2011). Despite its ability to break down many compounds, its ability to produce metabolites and their function is not as well-characterized. *V. paradoxus* strains can produce compounds such as N-acyl-D-amino acid amidohydrolase, D-amidase, and  $\alpha$ -methylserine aldolase, yet their role within the bacteria is not known (Satola et al., 2013).

Additionally, *V. paradoxus* has previously been investigated to discover novel natural products through both natural products chemistry and genome mining. It was analyzed to predict natural products from BGCs through a web-based tool called Genomes-to-Natural Products platform (Johnston et al., 2015). In this paper, the authors used their platform to predict metabolites from the bacteria through the NRPS/PKS gene cluster and then isolated novel nonribosomal peptides from two strains of *V. paradoxus*, strain S110 and strain P4B. A study done by Kurth et al. describes the identification of lipopeptide siderophores through genome mining of *Variovorax boronicumulans* (Kurth et al., 2016). Robertson et al. isolated and characterized the amphiphilic lipopeptide siderophore imaobactin from *Variovorax* sp. RKJM285 through natural products chemistry (Robertson et al., 2018).

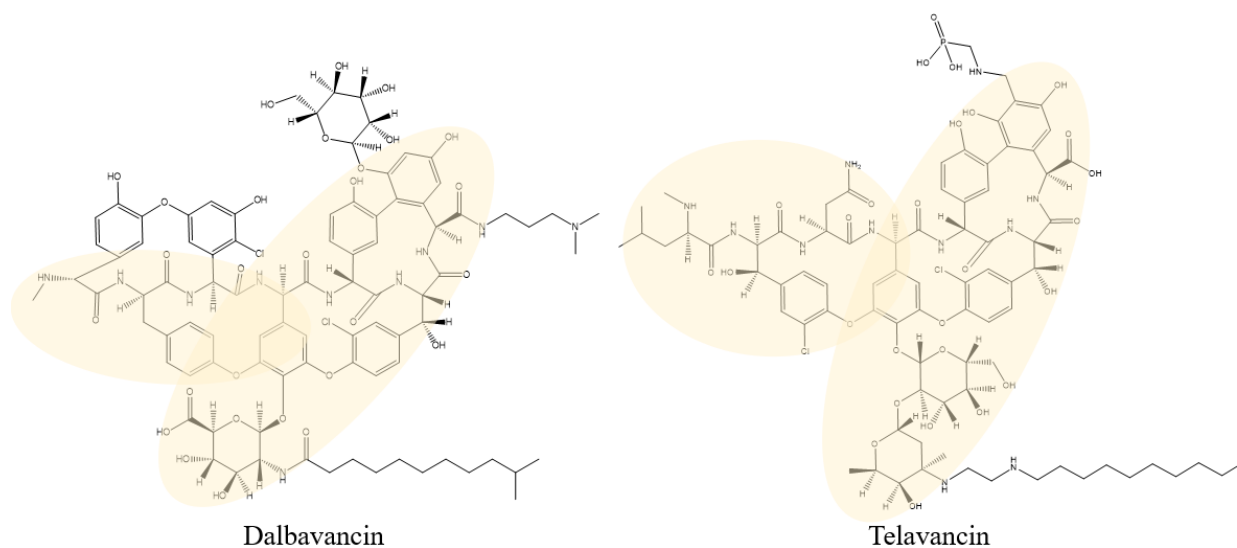
Like many other microorganisms, *V. paradoxus* is found in biofilms. *V. paradoxus* strain EPS (VP EPS) inhibited *S. aureus* biofilm formation when grown together in co-culture (Gomez, 2022). Furthermore, the filtered supernatants of the mono-culture *V. paradoxus* and in co-culture with *S. aureus* resulted in biofilm inhibition, suggesting this could be due to a small molecule

produced by *V. paradoxus*. The filtered supernatants were added to centrifugal filters with a molecular weight cut off of 10,000 Da and both supernatants (remained in the filter and passed through the filter) were tested for their biofilm inhibition activity. It was found that the supernatant that passed through the filter (MW less than 10,000 Da) caused biofilm inhibition, indicating the molecule was less than 10,000 Da. Upon further analysis, the MW of a glycolipopeptide was determined to be 1,007 Da.

### **2.1.3 Glycolipopeptides**

Glycolipopeptides (GLPs) are small molecules that consist of a sugar (glyco), lipid (lipo) and peptide component. GLPs are a class of amphiphilic biosurfactants due to the hydrophobic (lipid) and hydrophilic (sugar and polar amino acids) components of the molecule.

Biosurfactants reduce surface and interfacial tension to allow external nutrients to be taken in (Banat et al., 2014). Dalbavancin and telavancin are GLPs that are FDA-approved drugs for the treatment of complicated skin and skin structure infections in adults have also shown to inhibit *S. aureus* biofilms (Meeker et al., 2016). Figure 1 shows the structures of dalbavancin and telavancin. Both drugs are semisynthetic derivatives of vancomycin (Figure 1, highlighted in yellow) (Malabarba & Goldstein, 2005; Damodaran & Madhan, 2011). Vancomycin, a glycopeptide, was chemically modified to include a lipid chain and some side chains were substituted to produce dalbavancin and telavancin, which may be responsible for an increase in its antimicrobial potency (Malabarba & Goldstein, 2005; Das et al., 2017).



*Figure 1.* Structures of dalbavancin and telavancin. Both compounds are semisynthetic GLP derivatives of vancomycin. The vancomycin core is highlighted in yellow.

#### 2.1.4 Natural Products Workflow

The traditional approach to natural products chemistry is via bioassay-guided fractionation where a single isolated compound is pursued for the observed bioactivity (Atanasov et al., 2021; Wolfender et al., 2019). This workflow can be time-consuming and the isolation of a single bioactive compound is limited to the types of assays available and the amount of material required for each round of testing. Biological samples, either collected from the environment or cultured in the laboratory, are extracted using solvents of varying polarities. The product of the extraction step is called the crude extract and is rarely tested for bioactivity due to its complexity, as they can contain thousands of compounds. Crude extracts are usually either partitioned or fractionated to simplify the number of compounds. Liquid-liquid partitioning is commonly used to separate compounds by polarity. Polar compounds include salts, sugars, nucleic acids, whereas nonpolar compounds include lipids. Fractionation occurs via solid-phase extraction (SPE) or column chromatography with a variety of stationary phases, with Silica or C18 as the most common (Sarker et al., 2005). While fractionation will simplify the number of

compounds, multiple rounds of fractionation and bioactivity testing are necessary to isolate a single compound. Once an extract is fractionated, analytical techniques such as high-performance liquid chromatography (HPLC) can be used to analyze and isolate compounds. The final amount of a pure natural product obtained from an organism is usually very low, approximately 0.01 to 0.1 mg.

The loss of bioactivity and failure to isolate a bioactive compound through bioassay-guided fractionation is a major issue. Some reasons for this are the degradation of the bioactive compounds during purification, loss of material during fractionation, and the observed bioactivity may be due to the synergistic effects from the interaction of multiple compounds (Nothias et al., 2018). To resolve this, dereplication strategies were developed. Dereplication strategies allow natural products scientists to analyze less material faster, allowing for the detection of known compounds utilizing mass spectrometry data. For LC/MS, the mass injected is usually 0.001 mg, which is equivalent to 10  $\mu$ L of a 0.1 mg/mL solution. Web-based tools for dereplication were created which allow scientists to upload their data and search  $m/z$  values and MS/MS fragmentation patterns compared to databases for known compounds. Web-based tools and natural product specific databases (e.g., MarinLit, Antibase, and the Dictionary of Natural Products) have helped natural products scientists derePLICATE their data and to prioritize new compounds early in the natural products workflow (Nothias et al., 2018; Wolfender et al., 2019; Atanasov et al., 2021).

Natural product chemistry relies on many analytical techniques and instruments to isolate, purify, and identify a compound. If a fraction from a crude extract displays bioactivity, the first step is to look for known compounds based on the bioactivity data or the producing organism (if known, in the case of algae, cyanobacteria, etc.) using LC/MS. If no known

compound is found, the active fraction is further separated using HPLC. The structure of a pure compound can then be elucidated. Mass spectrometry (MS) is an analytical technique that is heavily used in natural products chemistry to dereplicate (discussed above), analyze unknown samples, quantify a known analyte, and start determining the compound by structural features (Throck Watson & David Sparkman 2007). Compounds analyzed via mass spectrometry are detected as ions and the mass-to-charge ratio ( $m/z$ ) is obtained by dividing the mass of the ion by the charge of the ion. The  $m/z$  value is then used to determine the molecular weight and structural features. The accurate molecular weight can be determined, and ultimately the molecular formula, via mass spectrometry because it uses exact masses of the most abundant isotopes of the elements present. The combination of chromatography and mass spectrometry (e.g., LC/MS) is often used to separate complex fractions for the deconvolution of mass spectra (Wolfender et al., 2019). Additionally, tandem mass spectrometry (MS/MS) can provide detailed structural information by means of fragmentation patterns of molecules. Each fragmentation pattern of a molecule is analogous to fingerprints that can then be used to piece the structure together.

### **2.1.5 Genome Mining**

Bacteria have been a prolific source of natural products for decades and have been a source of many therapeutic agents (Hug et al., 2020). Genome mining has become popular for drug discovery because genetic information allowed scientists to predict natural products based on DNA alone (Ziemert et al., 2016). Genome mining searches for biosynthetic gene clusters (BGCs) which encode for proteins that produce compounds or derivatives (Machado et al., 2017). A BGC is a group of two or more genes within one region that encodes for a biosynthetic pathway for the production of a metabolite (Medema et al., 2015). Bacteria produce metabolites,

at varying abundances, for intra- and extracellular signaling in response to changes in their environment (Camilli & Bassler, 2006). Compounds are predicted based on the assembly line of organized enzymes. The order of these enzymes dictates the sequence substrates are combined or modified, yielding an overall structure (Fischbach & Walsh, 2006).

The two most easily characterized BGCs are nonribosomal peptide synthetases (NRPS) and polyketide synthetases (PKS) (Boddy, 2014). The domains in NRPS and PKS are well-characterized. Their functions can be predicted with certainty because they are highly conserved which is observed in the similarity of amino acid sequences, despite the diversity of secondary metabolites produced (Boddy, 2014; Ziemert et al., 2016; Scherlach & Hertweck, 2021). NRPS are multimodular proteins that incorporate certain amino acids into the growing peptide (McErlean et al., 2019). The web-based platform antiSMASH (antibiotics and Secondary Metabolite Analysis SHell) is a widely used tool for mining, annotation, and analysis of microbial genomes for secondary metabolites (Blin et al., 2021). Within antiSMASH, BGCs are matched, the cluster type is identified, and the predicted compound from the BGC is displayed based on the proteins in the BGC. While the domain proteins in BGCs are conserved, the secondary metabolites they produce vary greatly due to substrate specificity.

Another database used for the prediction of natural products is MIBiG (Minimum Information about a Biosynthetic Gene Cluster) Data Standard and Repository. The MIBiG database allows users to adjust parameters, such as publications involving gene cluster characterization, genomic loci, chemical compounds from the encoded biosynthetic pathway (Medema et al., 2015). MIBiG is a fundamental reference database for BGCs with known functions and is used for comparative analyses within antiSMASH because it contains a standardized requirement of BGC annotations and gene cluster-associated metadata (Kautsar et



al., 2020; Medema et al., 2015). The combined use of antiSMASH and MIBiG with bioassay-guided fractionation can be useful for the discovery of novel compounds (Trivella & de Felicio, 2018).

## 2.2 Materials and Methods

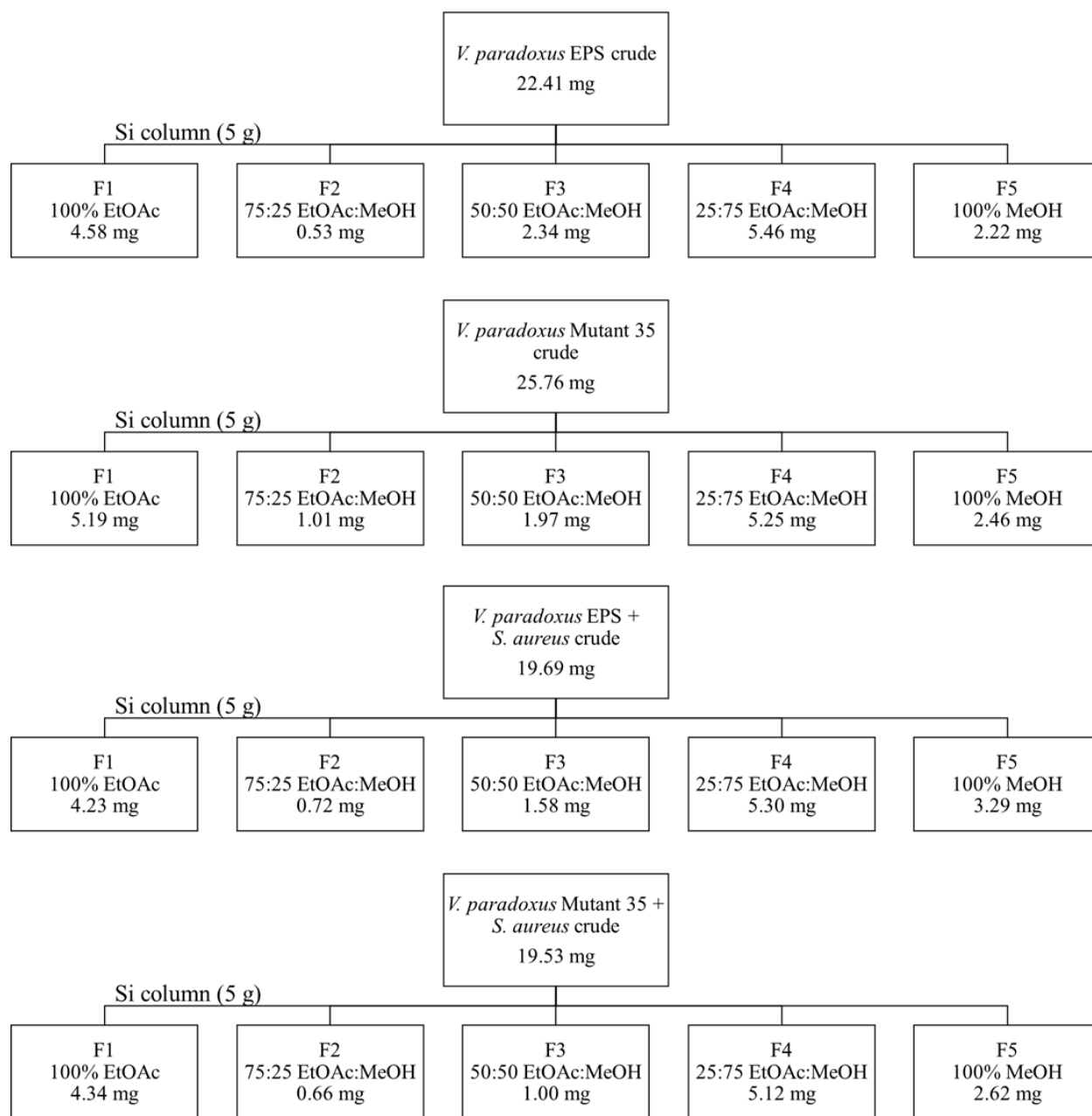
### 2.2.1 Bacterial Strains and Culture Conditions

Paul Orwin collection strains of *V. paradoxus* strain EPS (VP EPS), *V. paradoxus* strain  $\Delta$ 4519 (KmR) (VP Mut 35), *S. aureus* strain AH1710=*S. aureus* RN4220 + pCM29 CmR (PsarA\_RBSsod\_SGFP) were used in this study. Mono-cultures of VP EPS, VP Mut 35 and *S. aureus* were obtained following overnight growth at 30°C and shaking at 200 RPM. Co-cultures of VP EPS + *S. aureus* (V+S) and VP Mut 35 + *S. aureus* (35+S) were obtained following the biofilm assay for 48 h at room temperature as described in Gomez 2022. The cultures were centrifuged, the supernatant was saved, and the cell pellet was discarded. The supernatant was then syringe filtered (0.22  $\mu$ m) to remove bacterial cells before downstream assays and analysis.

### 2.2.2 Extraction and Fractionation

Filtered (0.22  $\mu$ m) 5 mL mono-cultures of VP EPS, VP Mut 35 and *S. aureus*, co-cultures of V+S and 35+S, and a YE media blank were extracted using 35 mL of a 2:1 CHCl<sub>3</sub>:MeOH solvent mixture. The crude extracts were concentrated *in vacuo* and weighed at 10 mg/mL in LC/MS MeOH prior to LC/MS analysis.

VP EPS, VP Mut 35, V+S, and 35+S crude extracts then were fractionated using Silica (5 g) Solid Phase Extraction (SPE) using 100% EtOAc, 75:25 EtOAc:MeOH, 50:50 EtOAc:MeOH, 25:75 EtOAc:MeOH, and 100% MeOH resulting in 5 fractions per culture (Figure 2). 20 mL of each fraction was eluted. The fractions were concentrated *in vacuo*, weighed, and resuspended in DMSO at 10 mg/mL for testing for biofilm inhibition.



**Figure 1.** Fractionation trees of crude extracts of the two mono-cultures and two co-cultures. The 0.22  $\mu$ m filtered media was extracted using a 2:1  $\text{CHCl}_3$ :MeOH solvent mixture and concentrated *in vacuo* to obtain a crude extract (crude). The crude extracts were then fractionated using Si (5 g) SPE column resulting in 20 mL per fraction eluted according to the tree above.

### 2.2.3 LC-MS/MS Data Analysis

Samples were analyzed using GNPS LC-MS Dashboard (Petras et al., 2022) for both MS1 and MS/MS data. The extracted ion chromatogram (XIC) tool was used to search for  $[M+H]^+$  1,008 due to the previous knowledge of the MW of the molecule. MS1 data was analyzed based on the retention time from the XIC at  $[M+H]^+$  1,008 and applied to the TIC to analyze the mass spectra. MS/MS spectral data for  $[M+H]^+$  1,008 was analyzed based on the retention time of the MS/MS acquisition.

### 2.2.4 Biofilm Inhibition Assay

Mono-culture of *S. aureus* was grown overnight in yeast extract (5 g/L) broth (YE) with chloramphenicol 0.03 g/L at 30°C, shaking at 200 RPM. The cell density was then measured using a Genesys 30 Visible Spectrophotometer (Thermo Scientific), with  $OD_{595} = 1$ . In a centrifuge tube, 1 mL of the culture was centrifuged, the supernatant was discarded, and the cells were washed in YE broth twice. The cells were then resuspended in 500  $\mu$ L of YE and then diluted 1:100 in YE for a final volume of 50 mL resulting in  $OD_{595} = 0.01$ . To each well of a 12-well plate, 500  $\mu$ L of diluted *S. aureus* culture was added. A total of 20 fractions were tested, along with unextracted mono- and co-culture media of VP EPS, VP Mut 35, V+S and 35+S as a positive control, DMSO as a vehicle control, and YE broth as a negative control. In the designated well, 5  $\mu$ L or 10  $\mu$ L of the fraction or control was mixed with diluted *S. aureus* culture to deliver 0.2 mg/mL of the compound. The plates were incubated for 24 h at room temperature at a slant using a 10-mL serological pipette to easily detect the biofilm.

After 24 h, the media was removed by placing the plate at the opposite angle. This ensured the biofilm was not disturbed when removing the culture fluid from the wells. The wells were rinsed twice with 1 mL of DI water to remove planktonic cells. Then 1 mL of 1% crystal

violet was then added to each well and left to sit for 15 minutes. After 15 minutes, the wells were washed with DI water to remove the crystal violet and left to dry for 15 minutes before observing the biofilm.

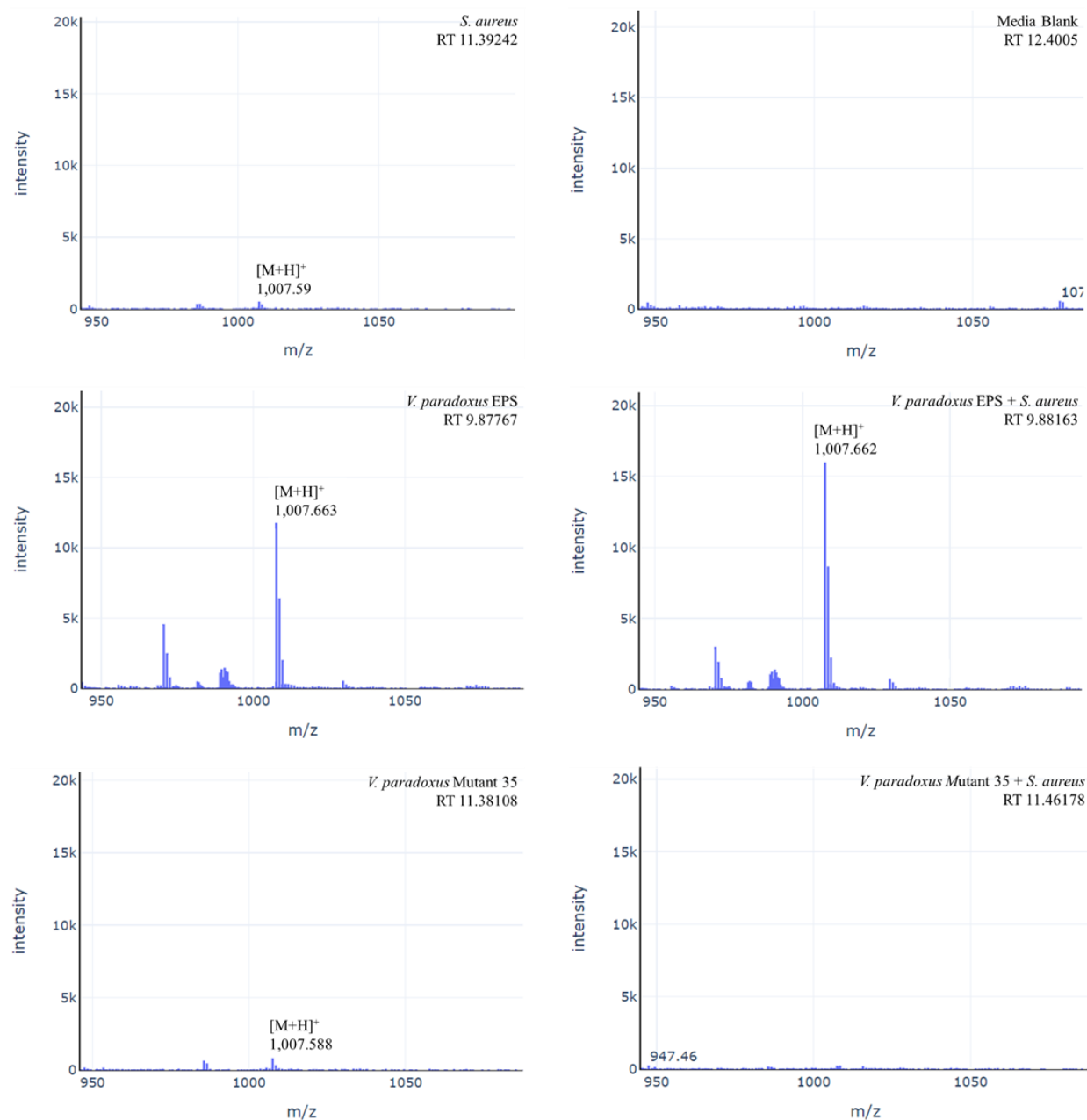
## 2.3 Results and Discussion

### 2.3.1 Extraction and LC-MS/MS on Crude Extracts

Filtered (0.22  $\mu\text{m}$ ) cultures of VP EPS, VP Mut 35 and *S. aureus* mono-cultures, V+S and 35+S co-cultures, and YE media blank were extracted using 35 mL of a 2:1  $\text{CHCl}_3$ :MeOH solvent mixture for each sample. These solvents were chosen to maximize the yield of the suspected GLP present in VP EPS and V+S based on the hydrophobic functional groups of the molecule. The crude extracts were concentrated *in vacuo* and weighed at 10 mg/mL in LC/MS MeOH. They were then analyzed via LC-MS/MS to determine if the GLP was present in VP EPS and V+S only. Figure 3 compares the MS1 mass spectral data based on the XIC of  $[\text{M}+\text{H}]^+$  1,008 of all crude extracts. Only VP EPS and V+S extracts show  $[\text{M}+\text{H}]^+$  1,008 with significant intensity, indicating this molecule is only present in these two extracts. The retention times of VP EPS and V+S extracts were similar at around 9.8 minutes, indicating the molecules eluted at similar solvent polarity may be the same. The other extracts had retention times past 11 minutes, indicating that they are likely not the same molecule as the molecule that eluted at 9.8 minutes. VP Mut 35 is a surfactant defective strain in which it does not produce the biosurfactant; thus, it is logical that VP Mut 35 and 35+S extracts showed no peaks at  $m/z$  1,008 with significant intensity as it does not have the capability to produce the surfactant (GLP).

MS/MS data was also collected and analyzed. VP EPS and V+S extracts had MS/MS acquisitions while the other extracts did not, indicating the GLP is significantly present in these two extracts. The MS/MS mass spectral data provides information on how a molecule

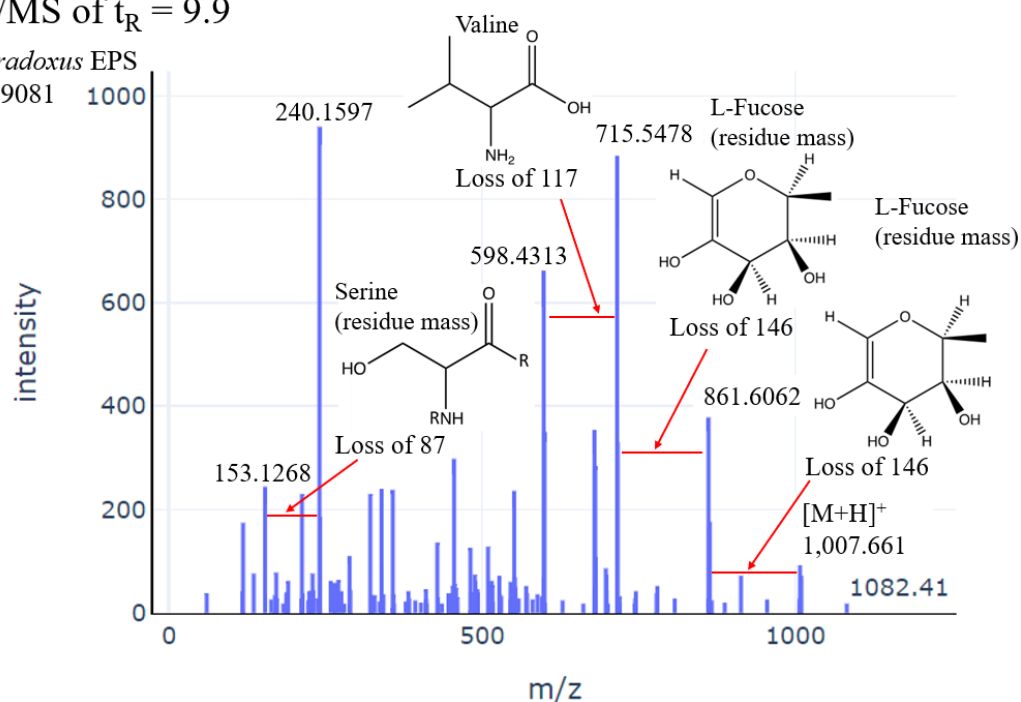
fragments, providing additional structural information. The unique fragmentation patterns of each molecule allows for the differentiation between molecules of the same mass. In Figure 4, the preliminary matches for  $m/z$  values are shown above the  $m/z$  loss. In both MS/MS mass spectra of VP EPS and V+S, the same mass losses were observed, indicating the same molecule is present in both extracts. The  $[M+H]^+$  ion was observed to be  $m/z$  1,007.66 for both extracts. The MW of the molecule is 1,007 Da but the protonated molecule has a  $m/z$  value of 1,007.66 which may be due to negative mass defect, which can cause the slight difference between the integer mass (1,007 Da) and the exact mass of a molecule (seen in the mass spectral data) (Sleno, 2012; Pleil & Isaacs, 2016). Noting the intensity of both spectra, VP EPS has a maximum intensity of 1,000 and V+S has a maximum intensity of 3,500 suggesting that the GLP production may be increased in the co-culture. The loss of two 146  $m/z$  units could represent the residue mass of L-fucose. Fucose is a deoxy hexose that lacks a hydroxyl group on the carbon in the 6th position of the ring. Additionally, VP EPS encodes for a protein called VARPA\_1431 which is predicted to be an alpha fucosidase, suggesting that fucose may be the sugar present in the molecule (Gomez, 2022). The loss of 117  $m/z$  units could represent the amino acid valine and the loss of 87  $m/z$  units could represent the residue mass of the amino acid serine. Various studies have found that D-amino acids have the ability to inhibit biofilms (Kolodkin-Gal et al., 2010; Hochbaum et al., 2011; Ramón-Peréz et al., 2014), indicating that the amino acids in the GLP may have a D-configuration and may play a role in biofilm inhibition.



**Figure 3.** Mass spectra comparison of crude extracts. Retention times were chosen based on the highest peak on the EIC searching for  $[M+H]^+$  1,008. Only VP EPS and V+S show significant intensity of  $[M+H]^+$  1,008 at similar retention times of 9.8 minutes. All other extracts had retention times past 11 minutes and no significant peaks of  $[M+H]^+$  1,008.

MS/MS of  $t_R = 9.9$ *V. paradoxus* EPS

RT 9.9081

MS/MS of  $t_R = 9.8$ *V. paradoxus* EPS + *S. aureus*

RT 9.88905

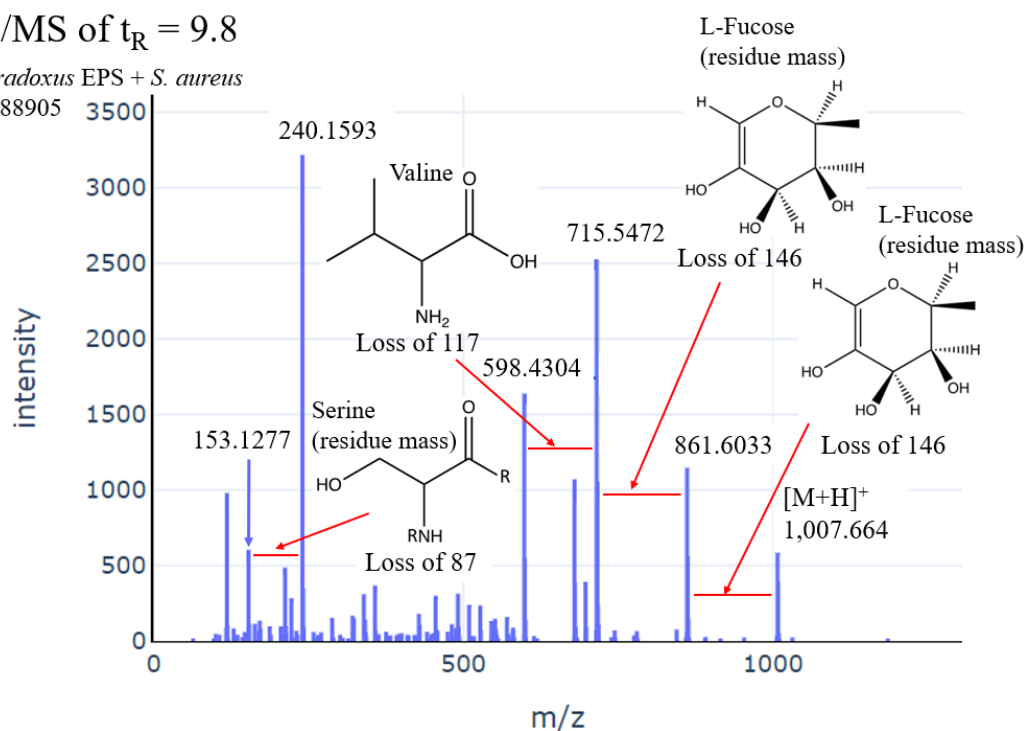


Figure 4. MS/MS spectra of VP EPS and V+S crude extracts. The  $m/z$  was specified at  $m/z$  1,008 for MS/MS acquisition. MS/MS acquisition was around 9.8-9.9 minutes for both extracts. The same mass losses were observed in both extracts. Loss of 146 represents the residue mass of L-fucose. Loss of 117 represents the amino acid valine. Loss of 87 represents the residue mass of the amino acid serine.



### 2.3.2 GLP Production by *V. paradoxus*

A 2019 patent describes a GLP from *V. paradoxus* strain RKNM-096, NB-RLP1006 (Kerr et al., 2019). Based on the similar  $m/z$  values, the GLP in this study is likely elementally and structurally similar to the GLP in the patent (Figure 5). The sugar groups are likely attached to the lipid chain through a glycosidic bond and the amino acids are likely attached covalently to the other side of the lipid chain. In the patent the sugar groups identified were rhamnose, however our data suggests that the sugar groups are likely L-fucose (Figure 4). However, the two sugars have the same mass of 164 Da and residue mass of 146 Da. To determine which sugar is incorporated, NMR of the molecule is needed. The patent reports the  $[M+H]^+$  ion at  $m/z$  1,007.6628, and our MS/MS  $[M+H]^+$  ion at  $m/z$  1,007.664 (Figure 4). Based on the structure given in the patent, its molecular formula is  $C_{51}H_{94}N_2O_{17}$ . The molecular formula of the GLP in this study is hypothesized to be  $C_{51}H_{95}N_2O_{17}$ . The patent then continues to describe synthesis and semi-synthesis of structurally similar GLPs and the cytotoxicity of the molecule.

The extraction method described in the patent was different from what was done in this study. In the patent, *V. paradoxus* RKNM-096 was grown in ISP2 media at 30°C for five days. After five days, the cells were removed by centrifugation and the supernatant was mixed with kerosene, vortexed, and incubated overnight at room temperature. The mixture was then extracted twice using 10 mL of EtOAc. The EtOAc extract was then partitioned with water to remove polar media components. The extracts were separated using a UHPLC and analyzed using a high-resolution mass spectrometer utilizing electrospray ionization. In this study, 0.22  $\mu$ m filtered cultures were extracted using a 2:1  $CH_3Cl$ :MeOH solvent mixture. The extracts were then separated using a UHPLC and analyzed by trapped ion mobility spectrometry coupled with time-of-flight mass spectrometry. Despite the different extraction and analysis methods, a GLP

was detected in both the patent and in this study. The structure of the GLP in the patent was determined via MS and NMR.

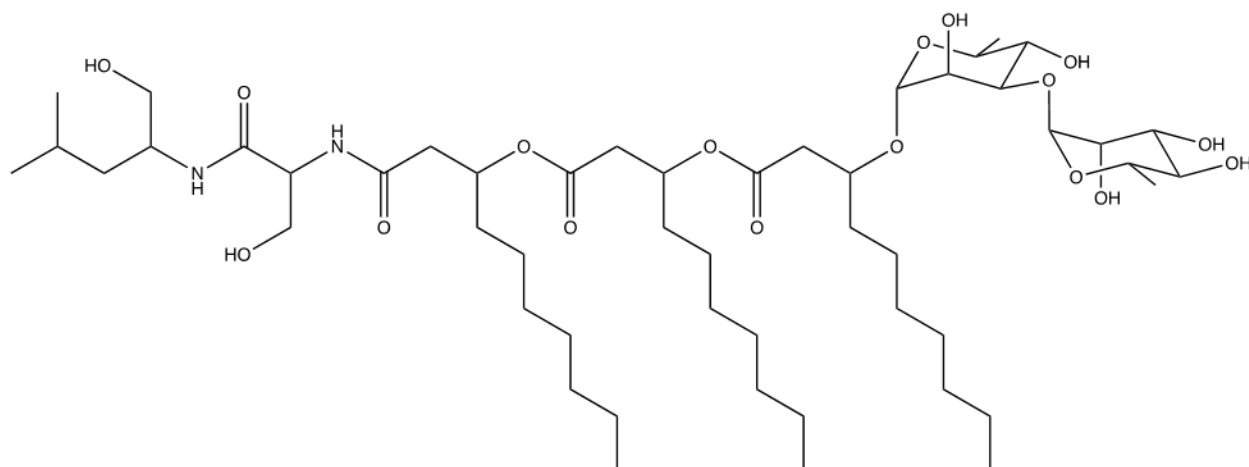


Figure 5. Structure of NB-RLP1006, a GLP from *V. paradoxus* RKNM-096.

Additionally, the patent provided genetic information of the bacteria. The amino acid sequence of the NRPS in the patent and this study were aligned using Clustal Omega (Figure 6) (Maderia et al., 2022). While many of the amino acids align as designated by an asterisk (\*), there are many places where they do not align. A colon (:) represents amino acids that have strongly similar properties, a period (.) represents amino acids with weakly similar properties, and a blank space represents two different amino acids (Madhusoodanan, n.d.). The differences in amino acids indicates the protein may recruit different substrates into the 2-amino acid peptide.

V_paradoxus_EPS	MSTVDQLGRTAPLTSGQMAMWLGAKFASPDNFNLAEAIDIAGEIDPDIFLAAMRQVADE
V_paradoxus_RKNM-096	MSTVDQLGRTAPLTSGQMAMWLGAKFASPDNFNLAEAIDIAGEIDPAIFLAAMRQVADE
	*****
V_paradoxus_EPS	VEATRLGFVDTQPGRQVVAPVFAGEIPYLDLSGSDPLAEAERWMRADYTRNIDLAHQG
V_paradoxus_RKNM-096	VEATRLSFIDTPQGRQVVAPVFTGEIPYLDLSGESDPQAEAEERWMHADYTRSIDLAHQG
	*****.*:*****.*:*****.*:*****.*:*****.*:*****.*:*****
V_paradoxus_EPS	LWLSALIRLAPDRHIWYHRSHHIVLDGFSGGLIARRFADTYTAMADDNAAVPEDSRLAPI
V_paradoxus_RKNM-096	LWLSALIRLAPDRHIWYHRSHHIALDGFSGGLIARRFADITYTAMVDNNAAVPEDSRLAPI
	*****.*:*****.*:*****.*:*****.*:*****.*:*****.*:*****
V_paradoxus_EPS	SQLADEEHAYRESGRFPRDRQYWTERFADAPDPLSLASRRSVNIGGLLRQTVHLPAASVQ
V_paradoxus_RKNM-096	SQLADEEHAYRESGRFPRDRQYWTERFADAPDPLSLASHRSVNVGGLLRQTVHLPAASVQ
	*****.*:*****.*:*****.*:*****.*:*****.*:*****.*:*****
V_paradoxus_EPS	ALQTIAQELGTTLPQILIATTAAYLYRATGIEDMAIGIPVTARHNDMRMRVPAMVANALP
V_paradoxus_RKNM-096	ALQTIAQELGTTLPQILIATTAAYLYRATGIEDMAIGIPVTARHNDMRMRVPAMVANALP
	*****
V_paradoxus_EPS	LRLAMRADLPIPELIREVGRQMRQILRHQSYRYEHLRSDLNMLVNNRQLFTTVVNEPFD
V_paradoxus_RKNM-096	LRLAMRADLPIPELIREVGRQMRQILRHQSYRYEHLRSDLNMLVNNRQLFTTVVNEPFD
	*****
V_paradoxus_EPS	YDFRFAGHPAKPRNLSNGTAEDLGIFLYERGNGQDLQIDFDANPAVHTAEDLADHQRRLL
V_paradoxus_RKNM-096	YDFRFAGHAALPRNLSNGTAEDLGIFLYERGNGQDLQIDFDANPAVHTAEELADHQRRLL
	*****.*:*****.*:*****.*:*****.*:*****.*:*****.*:*****
V_paradoxus_EPS	AFIDAVIRLPLQAVGQIDLLGADERKQLLVTWNDTAHTVPDMHLTALIEAQLAANPQAI
V_paradoxus_RKNM-096	AFIDAVIRLPLQAVGQIDLLGAERQQLLVEWNTAHAVPDTHLTALIEAQLAADPQAI
	*****.*:*****.*:*****.*:*****.*:*****.*:*****.*:*****
V_paradoxus_EPS	LRFDGEAMPNEELNRRANRLAHLRARGAGPERTVALAIPRSMMLMALLATLKTGAAYL
V_paradoxus_RKNM-096	LRFDGEAMNNEELNRRANRLAHLRARGAGPERTVALAIPRSMMLMALLATLKTGAAYL
	*****.*:*****.*:*****.*:*****.*:*****.*:*****.*:*****

**Figure 6.** Amino acid sequence alignment of *V. paradoxus* EPS and *V. paradoxus* RKNM-096. Symbols below both sequences represent similarity in amino acid character. An asterisk (\*) represents the same amino acid in both sequences, a colon (:) represents amino acids with strongly similar properties, and a period (.) represents amino acids with weakly similar properties. A blank space represents two different amino acids. This figure shows the first 540 amino acids of both sequences.

### 2.3.3 Fractionation and Biofilm Inhibition Assay

Consequently, the partially characterized GLP is not responsible for the biofilm inhibition activity. VP Mut 35 and 35+S crude extracts were included in fractionation because biofilm inhibition was observed in by VP Mut 35 (Gomez, 2022). VP EPS, VP Mut 35, V+S, and 35+S crude extracts were fractionated using Silica (5 g) SPE resulting in five fractions per culture (Figure 2). Biofilm inhibition was observed in the four cultures, thus they were selected for

fractionation. Through bioassay-guided fractionation, the bioactive molecule responsible for biofilm inhibition can be identified.

Fractions were concentrated at 10 mg/mL in DMSO for testing for biofilm inhibition. To approximate the concentration of the compound VP EPS produced, the natural concentration was calculated by dividing the mass of the fraction (1 mg) and the total volume extracted (5 mL). This resulted in a concentration of 0.2 mg/mL required to be added to each well, which is equivalent to 20  $\mu$ L of the 10 mg/mL solution. The final concentration of DMSO was 0.1%. This volume was not selected because the DMSO tolerance of VP EPS and *S. aureus* is not known. Instead, 5 or 10  $\mu$ L were used to observe the DMSO tolerance and to examine if biofilm inhibition occurs at a lower amount.

Based on the results from the biofilm inhibition assay, the fractions that caused biofilm inhibition will then be separated further using HPLC. These subfractions will then be retested for biofilm inhibition, ideally leading to the isolation of the bioactive compound. Once the bioactive compound has been isolated, the structure will be elucidated via NMR and MS.

#### **2.3.4 Genome Mining using antiSMASH**

antiSMASH was used to search for natural products encoded in DNA by analyzing the genome from VP EPS (Figure 7) (Blin et al., 2021). Eight BGCs were identified within the VP EPS genome that were further classified into the type of BGC (e.g., NRPS, PKS). Figure 7 gives the well-characterized natural product of the most similar BGC (MIBiG database), the natural products class, and the percent similarity of the BGC are given. Region 8 was selected for further analysis because VP Mut 35 was shown to be in this region. The eighth BGC contains an NRPS cluster type and the most similar known cluster produces bacillibactin, which is a

nonribosomal peptide, with a 15% similarity. The similarity is too low to be a definitive match and a more detailed comparative analysis of the eighth BGC to the MIBiG database was done.

The core biosynthetic gene within the eighth BGC is a NRPS, Varpa 4519 (Figure 8). Varpa 4519 consists of two modules that encode for a 2-amino acid peptide. The condensation domain (C) is located at the N-terminus and catalyzes amide bond formation, the adenylation domain (A) plays a role in peptide biosynthesis by catalyzing a two-step reaction, and the peptidyl carrier protein domain (PCP) is used to carry substrates and peptide intermediates between domains (B. Miller & Gulick, 2016). The terminal reductase domain is abbreviated as TD, will cleave the peptide from the enzyme (Figure 8). In the MS/MS data, a loss of 87  $m/z$  units was observed which could represent the residue mass of serine. Based on homology with other domains, the second amino acid was predicted to be one of the following: glycine, alanine, valine, leucine, isoleucine,  $\alpha$ -aminobutyric acid, isovaline. From the MS/MS data valine was hypothesized, but from the patent leucinol was determined to be the second amino acid. Valine, leucinol and isovaline all have a mass of 117 Da, suggesting the possibility of these three amino acids could be produced by VP EPS. Furthermore, there are other genes in the BGC that produce compounds that may be incorporated into the GLP. For instance, there is a glycosyltransferase and rhamnosyltransferase to the left of Varpa 4519, indicating the sugar in the GLP may not be fucose. To determine the rest of the structure, NMR of the compound is required.

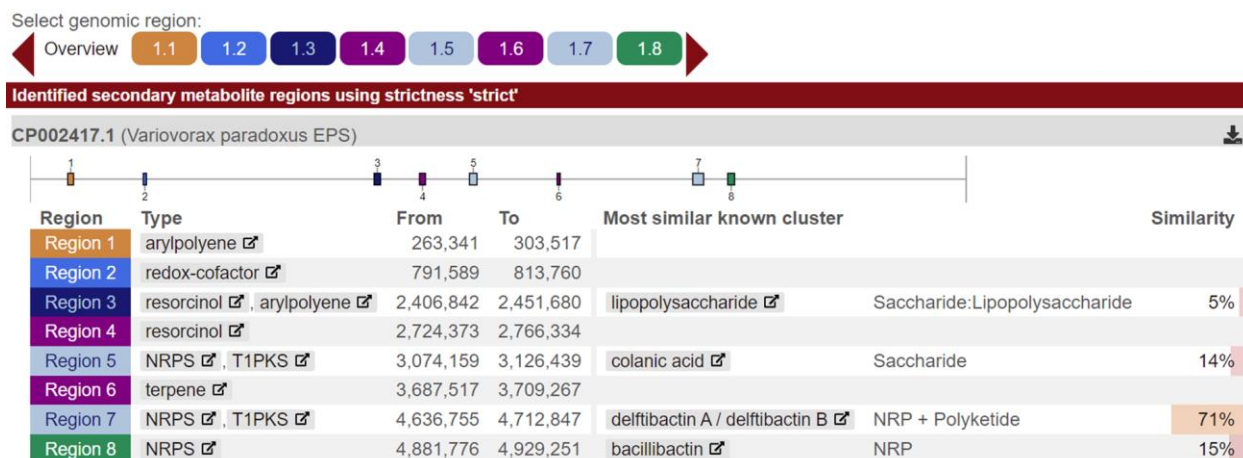


Figure 7. antiSMASH of *V. paradoxus* EPS. There are eight BGC regions identified in *V. paradoxus* EPS. Each BGC region is further classified into cluster types, labeled next to the region. The well-characterized natural product with the most similar BGC compared to the MIBiG database, the class of natural product, and the percent similarity are displayed on the right. The eighth BGC was selected for further analysis to attempt to identify the GLP due to the surfactant gene present in the eighth BGC. This figure was obtained from the antiSMASH website (Blin et al., 2021).

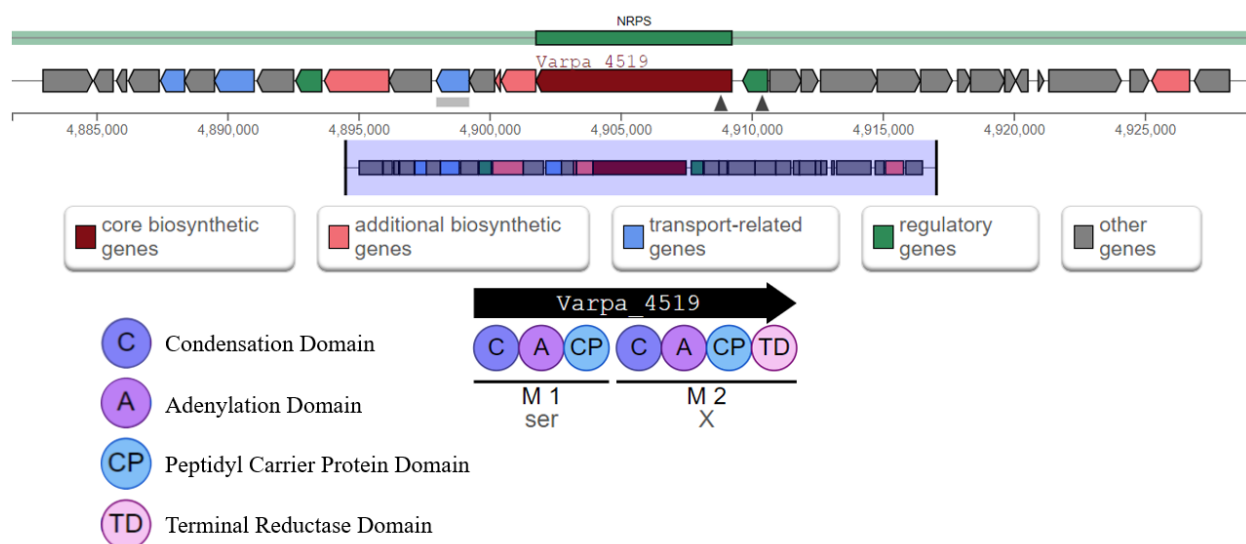


Figure 8. antiSMASH results of eighth BGC cluster from VP EPS. The core biosynthetic gene in the BGC is identified as a NRPS, Varpa\_4519. Varpa\_4519 is an amino acid adenylation domain protein that produces a 2-amino acid peptide. This figure was obtained from the antiSMASH website (Blin et al., 2021).

The gene Varpa 4519 was searched against the MIBiG database to see if any known natural products have similar BGCs (Medema et al., 2015). Table 1 displays the top ten results obtained from the search. The top result has a % ID of 48% and % Coverage of 84.3%, indicating the gene sequence similarity between the BGCs are relatively low despite the high coverage between them. The Expect value (E-value) which represents the number of hits that are expected when searching the database and decreases exponentially as the score of the match increases. Interestingly, the top ten results all have an E-value of 0.0, indicating the match is significant. However, identical short alignments have high E-values because the algorithm takes the length of the query sequence into account (“U.S. National Library of Medicine,” n.d.). Therefore, despite an E-value of 0.0, the short alignments may occur in the database by pure chance.

Table 1  
*MIBiG Hits of Varpa 4519*

Description of MIBiG Protein	Compound	Activity/Function	% ID	% Coverage	BLAST Score	E-value
Nonribosomal Peptide Synthetase (NRPS)	Paenibactin	Catechol-peptide siderophore	48	84.3	1804.0	0.0
Atr23	Atratamycin	Antibacterial activity against <i>M. tuberculosis</i> H37Ra and H37Rv	47	89.1	1785.0	0.0
Siderophore 2,3 Dihydroxybenzoate Glycine threonine Trimeric Ester Bacillibactin Synthetase	Bacillibactin	Catechol-based siderophore	46	85.5	1761.0	0.0
DhbF	Bacillibactin	Catechol-based siderophore	45	85.4	1688.0	0.0
CDA Peptide Synthetase I (CdaPs1)	Lipopeptide 8D1-1/2	Antimicrobial activity against <i>S. aureus</i>	45	89.0	1681.0	0.0
NRPS	Acyldepsipeptide 1	Antibiotic activity	45	85.7	1679.0	0.0
NRPS	Peptidocinnamin E	Farnesyl-transferase inhibitors	47	79.2	1651.0	0.0
CdaPs1	CDA1b/2a/2b/3a/3b/4a/4b	Calcium-dependent antibiotics	44	91.2	1647.0	0.0
WAPS1	WAP-8294A2	anti-MRSA activity	46	84.8	1642.0	0.0
Atr21	Atratamycin	Antibacterial activity against <i>M. tuberculosis</i> H37Ra and H37Rv	46	85.1	1621.0	0.0

*Note.* Table 1 only represents the top ten results.

## 2.4 Summary

A GLP was partially characterized in both VP EPS and V+S crude extracts through LC-MS/MS. A 2019 patent describing a GLP produced by *V. paradoxus* RKNM-096 provides hints toward the structure of the GLP produced by VP EPS. The patent provides strong implications of very similar structures that the LC-MS/MS data alone cannot prove any differentiations, despite the patent not exactly matching the genetic data from this study. Fractions of the crude extracts are being tested in a biofilm inhibition assay to identify bioactive fraction(s) for further separation and isolation of the bioactive molecule. The eighth BGC of VP EPS was analyzed through antiSMASH to assist in the characterization of the GLP and the MIBiG database to observe compounds from similar BGCs.



## CHAPTER 3: IDENTIFICATION OF CULTURABLE *CAULERPA* SPP.

### SURFACE-ASSOCIATED BACTERIA

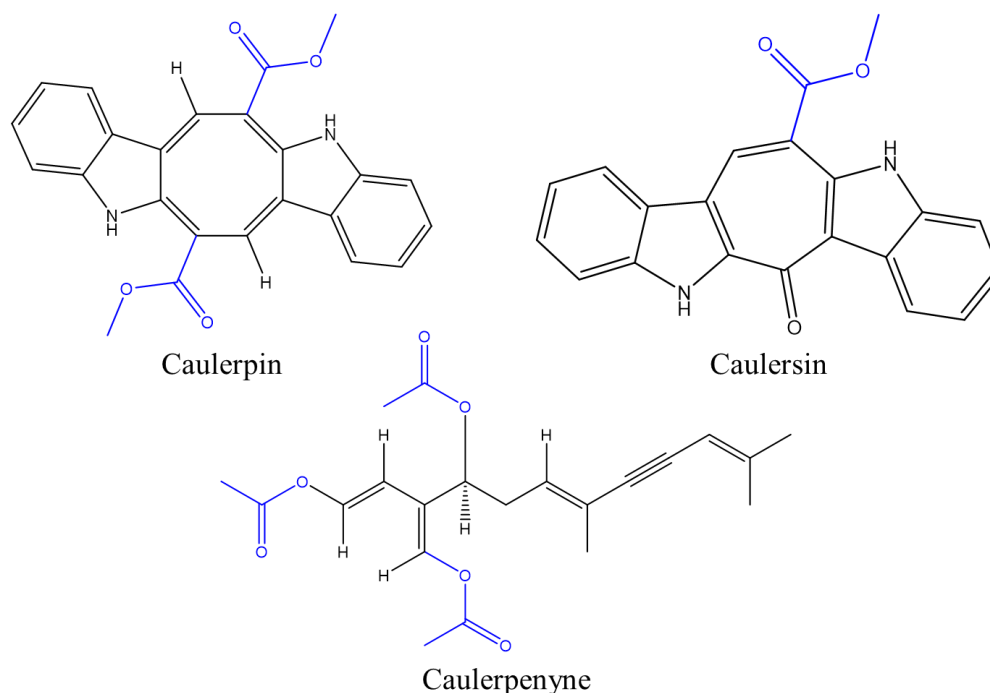
#### 3.1 Background

##### 3.1.1 *Caulerpa* spp.

The macroalgae genus *Caulerpa* are native to tropical and subtropical oceans (Mehra et al., 2019). *Caulerpa* spp. are common in residential in aquariums due to their aesthetics and easy propagation (Walters et al., 2006). Due to global warming, the temperature of oceans continues to rise at higher latitudes, allowing *Caulerpa* spp. to inhabit non-native environments (Walters et al., 2006; Montefalcone et al., 2015). Historically, it has been hypothesized to be an invasive species, dominating non-native regions by reproducing rapidly and colonizing available surfaces, outcompeting native organisms (Rizzo et al., 2016). In addition to this, the invader threatens native organisms by exerting adverse effects on the surrounding environment and the associated microbial communities, and negatively impacting native fish growth and population dynamics as a result of its invasiveness (Pierucci et al., 2019). Paul & Fenical discuss the various secondary metabolites produced by *Caulerpa* spp. that have significant toxicities to surrounding organisms hypothesized to be chemical defenses (Paul & Fenical, 1986).

Secondary metabolites produced by *Caulerpa* spp. are mostly composed of linear or monocyclic terpenes with aldehyde and characteristic enol-acetate functional groups (Mehra et al., 2019). Figure 9 shows some of the known secondary metabolites produced by *Caulerpa* spp., with these keystone enol-acetate functional groups highlighted in blue. Known secondary metabolites produced by *Caulerpa* spp. have been isolated following human-centric biological activities, such as cytotoxicity, antimicrobial, antiviral, and antifungal activities (Mehra et al.,

2019; Rushdi et al., 2020). *Caulerpa* spp. produce these secondary metabolites in the context of their surroundings, indicating they have a significant ecological role that remains unexplored.



*Figure 9.* Known abundant secondary metabolites produced by *Caulerpa* spp.. The characteristic enol-acetate functional groups are highlighted in blue.

Previous studies indicate that macroalgal extracts regulate the settlement and colonization of bacteria on its surface (Goecke et al., 2010; Sneed and Pohnert, 2011; Salaün et al., 2012). To understand the spread and invasion in non-native environments, the chemical cues for the recruitment of bacteria to its surface needs to be studied (Aires et al., 2015; Arnaud-Haond et al., 2017). It is suggested that *Caulerpa* spp. produces secondary metabolites that are crucial in the formation of its bacterial community (Dobretsov et al., 2006). We propose that macroalgal-bacterial interactions are chemically mediated. Secondary metabolites produced by these macroalgae are hypothesized to be responsible for the regulation of settlement of surface-

associated bacteria (Steinberg et al., 2002; Puglisi et al., 2014). The aim of this study was to identify the culturable surface-settled bacteria through identification of the 16S rRNA gene to understand the chemical mediation of *Caulerpa* spp.. A total of 35 bacterial strains isolated from the surface of *Caulerpa* spp. collected from the Florida Keys were profiled.

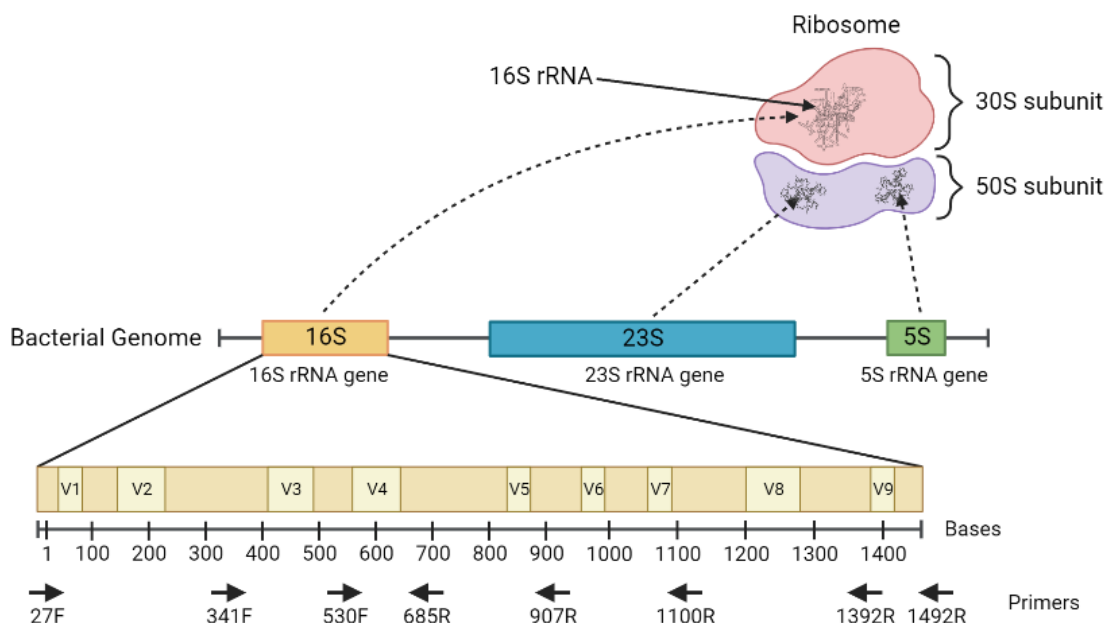
### 3.1.2 *Vibrio* spp. and Vibriosis

*Vibrio* spp. are Gram-negative bacteria that are commonly found in the marine environment. *Vibrio* spp. are known pathogens to both humans and marine organisms that can cause infections that can develop into fatal diseases (Thompson et al., 2004; Stocker & Seymour, 2012; Vezzulli et al., 2013). The most common infection is cholera caused by *Vibrio cholerae* (Baker-Austin et al., 2018). However, vibriosis, caused by non-cholerae *Vibrio* spp., can occur by wound exposure in seawater or consumption of contaminated raw or undercooked seafood (Baker-Austin et al., 2018). Rising temperatures in the oceans due to global warming favors the dispersal of *Vibrio* spp. and increased infections, with 320,000 cases predicted per year by 2030 (Baker-Austin et al., 2018; Sheahan et al., 2022).

*Vibrio* spp. are of interest to this project because they may play a role in protecting *Caulerpa* spp. due this pathogenicity (Rizzo et al., 2016). Some *Vibrio* spp. have been identified to be associated with algal surfaces through culture-dependent methods (Franco et al., 2020). Our hypothesis is that *Caulerpa* spp. recruits a higher percentage of *Vibrio* spp. to its surface. The ratio of Gram-positive to Gram-negative bacteria on the surface of algae compared to the surrounding seawater has been found to be distinct which may be due to the algal metabolites (Steinberg et al., 2002).

### 3.1.3 Bacterial Identification

The process of identifying isolated environmental bacterial strains includes the following steps: 1) genomic DNA extraction, 2) amplification of the 16S rRNA gene, 3) cleanup, 4) sequencing, and 5) curation of sequencing data for identification. The 16S rRNA gene is used for bacterial identification because: 1) the 16S rRNA gene is present in all bacteria, 2) the function of the gene is consistent and changes in the sequence is indicative of million years of evolution, and 3) the size of the gene (1,500 bp) is large enough for statistical purposes for sequence divergence (Patel, 2001). This 1,500 bp region is considered a fingerprint for the identification of bacterial strains. The 16S rRNA gene is used for identification because it has a highly conserved region that all bacteria encode for (Fukuda et al., 2016). The 16S rRNA region consists of ten regions, one conserved region and nine hypervariable regions which differentiates bacterial genus and sometimes species due to the sequence divergence in the hypervariable regions (Figure 10) (Van de Peer et al., 1996; Chakravorty et al., 2007). Primers are used to attach to the highly conserved regions, targeting the hypervariable regions for amplification (Figure 10).



Created in BioRender.com 

*Figure 10.* 16S rRNA gene. This region consists of ten regions, one conserved region and nine hypervariable regions which can differentiate bacterial genus and sometimes species. The primers used to attach to the 16S rRNA gene are considered universal primers because they target highly conserved regions, displayed on the bottom.

Polymerase chain reaction (PCR) is an established method to amplify a specific region of DNA. The three steps in PCR are: 1) denaturation, 2) annealing, and 3) elongation. These three steps are repeated approximately 30 cycles, to allow for sufficient amplification. One PCR cycle will double the targeted sequence, and after 30 cycles the targeted sequence is sufficiently amplified by a factor of millions. Each step requires its own temperature; denaturation requires 95°C, annealing temperature is primer dependent, and elongation requires 72°C programmed in a thermal cycler. In the denaturation step, the high temperature will cause the double-stranded DNA to unwind into single-stranded DNA, exposing the nucleotides. The annealing step involves the attachment of primers to their complementary bp to the single-stranded DNA, and

the elongation step attaches free-floating dNTPs to the DNA template via DNA polymerase forming double-stranded DNA. PCR products are then evaluated through gel electrophoresis, comparing the length of amplified DNA to a DNA ladder of known bp lengths.

Once the desired PCR product length is obtained, free-floating dNTPs, primers, polymerase and salts are removed. Cleaned PCR product is subjected to Sanger sequencing. Sanger sequencing involves the use of one primer and the addition of fluorescent ddNTPs (Sanger et al., 1977). ddNTPs lack the 3'-OH group which is found in dNTPs allowing the next nucleotide to form a bond; the lack of the 3'-OH group in ddNTPs prevents nucleotides from being added to the chain. Based on the different fluorescence of each ddNTP, the sequence of the 16S rRNA gene can be visualized on chromatograms and the sequence can be determined. The decoded sequence is then uploaded onto BLAST to search against the NCBI database to identify the bacterial strain.

#### **3.1.4 Agar Typing of Marine Bacteria**

Historically, the identification of bacterial strains can also be done based on growth or morphology on agar. A1 agar is used to grow and isolate marine bacterial strains because it is a high nutrient marine agar. Thiosulfate-Citrate-Bile Salts-Sucrose (TCBS) agar can be used for the identification of *Vibrio* spp.. TCBS agar is a selective media for the identification of *Vibrio* spp. due to the alkaline pH, high salt content, and addition of thymol and bromophenol blue which allows for differentiation between sucrose-using species (Letchumanan et al., 2014). *Vibrio* spp. that use sucrose form yellow colonies and those that do not form green colonies, narrowing down the species of *Vibrio* spp. (Thompson et al., 2004). MacConkey agar (MC) is a differential and selective media that inhibits the growth of Gram-positive bacteria, allowing Gram-negative bacteria (e.g., *Vibrio* spp.) to grow. Gram-positive bacteria are inhibited due to

the crystal violet and bile salts in MC agar (Jung & Hoilat 2021). Most *Vibrio* spp. are able to grow on MC agar due to their ability to ferment lactose (Brennan-Krohn et al., 2016). Growth on TCBS and MC agar allows for the morphological identification of *Vibrio* spp..

## **3.2 Materials and Methods**

### **3.2.1 Bacterial Isolation**

Bacterial strains were isolated from diversity plates of the surface-associated bacteria of *Caulerpa* spp. collected from the Florida Keys. Isolated bacterial strains were chosen for uniqueness based on their morphological appearance on A1 agar. Each isolated bacterial strain was given a name using the scheme 'C\_##' in which C represents *Caulerpa* spp., the underscore represents the specific *Caulerpa* species the bacteria was isolated from, and ## is the number assigned to the isolate. Isolates were then plated on TCBS agar plates to identify if they were *Vibrio* spp.. Isolates were grown in A1 liquid media and then cryo-preserved (final concentration 30% glycerol) for storage at -80°C until further analysis.

### **3.2.2 DNA Extraction**

Isolated bacterial strains are grown on A1 agar plates from -80°C stocks to confirm their purity. A single colony from a pure plate was inoculated in 2 x 4 mL of A1 media broth. A media only tube with no bacteria was also prepared to ensure the A1 media was not contaminated after overnight growth. The tubes are then put in a New Brunswick™ Excella® E24 Incubator Shaker Series (Eppendorf) at 180 RPM at 30°C for 12-18 h. The growth of each tube was evaluated by visual inspection of turbidity of the culture before DNA extraction. The bacterial culture was pipetted 1 mL at a time into a centrifuge tube, centrifuged for 4 minutes at 13,000-16,000 xg using a Centrifuge 5420 (Eppendorf), and the supernatant was discarded. This step was repeated for each bacterial strain.

DNA extraction was performed using the Wizard® Genomic DNA Purification Kit, following the Gram-Negative Bacteria Protocol with a few adjustments. Longer centrifugation times were used at the protein precipitation, DNA precipitation and rehydration steps (4 minutes), and the final volume for DNA rehydration was decreased to 50-100  $\mu\text{L}$ . The DNA concentration is checked using a NanoDrop™ 2000 Spectrophotometer and NanoDrop™ One Microvolume UV-Vis Spectrophotometer (Thermo Scientific). DNA extracts that had concentrations above 70 ng/ $\mu\text{L}$  and a 260/280 value above 1.7 were stored at  $-20^{\circ}\text{C}$  until further analysis. Extracted DNA below this concentration were discarded and the process was repeated.

### **3.2.3 PCR**

PCR was performed using a T100™ Thermal Cycler (Bio-Rad) and a Mastercycler® Personal (Eppendorf). Different primers were used to target different genes, specified in Table 1. For a final volume of 50  $\mu\text{L}$  per reaction, 1  $\mu\text{L}$  of extracted genomic DNA, 0.5  $\mu\text{L}$  of FC27, 0.5  $\mu\text{L}$  of RC1492, 0.5  $\mu\text{L}$  of dNTPs, 10  $\mu\text{L}$  of 5X Phusion HF Buffer (ThermoFisher), 0.5  $\mu\text{L}$  of Phusion DNA Polymerase (ThermoFisher), and 37  $\mu\text{L}$  of molecular-grade water were added to one PCR tube. For a negative control, molecular-grade water was used in replace of extracted genomic DNA. Thermal cycling steps were: 1) initial denaturing for 45 seconds at  $95^{\circ}\text{C}$ , 2) 30 seconds at  $95^{\circ}\text{C}$ , 3) annealing for 30 seconds at  $55^{\circ}\text{C}$ , 4) elongation for 45 seconds at  $72^{\circ}\text{C}$ , 5) steps 2-4 repeated for 30 cycles, and 6) final elongation for 5 minutes at  $72^{\circ}\text{C}$ .

The length of PCR product was confirmed using gel electrophoresis with a 1% agarose gel, 1  $\mu\text{L}$  of PCR sample with 5  $\mu\text{L}$  of loading dye were loaded it into each well and compared to a 1 kb DNA ladder (GoldBio). Gel electrophoresis was run using a Mini-Sub Cell GT Horizontal Electrophoresis System and PowerPac Basic Power Supply (Bio-Rad). Gel



electrophoresis was run at 120V for 35 minutes. Gel imaging was done using a ChemiDoc XRS+ Imaging System (Bio-Rad) and analyzed through Image Lab™ Software (Figure 12).

PCR products of the correct bp size when compared to the ladder were then cleaned up using GeneJET PCR Purification Kit (Thermo Scientific) following the manufacturer's protocol with a few adjustments. In the first step, a 2:1 ratio was used for binding buffer to PCR mixture rather than a 1:1 ratio and the final volume for elution was 25-50 µL compared to 50-100 µL. The concentration of cleaned PCR was measured using a NanoDrop™ One/OneC Microvolume UV-Vis Spectrophotometer (Thermo Scientific). The required concentration of cleaned PCR product was 40-60 ng/µL for sequencing.

Table 2  
*PCR primers to target specific genes*

Gene Target	Primer	Sequence (5' → 3')	Product Size (bp)	Reference
16S rRNA	FC27	AGAGTTTGATCCTGGCTCAG	1,500	Weisburg et al., 1990
	RC1492	TACGGCTACCTTGTACGACTT		
toxR	UtoxR	GASTTTGTTTGGCGYGARCAAGGTT	640	Bauer and Rørvik, 2007
	vctoxR	GGTTAGCAACGATGCGTAAG		
hsp60	Vib-hspF3-23	GAACCCNATGGAYCTKAARCG	420	King et al., 2019
	Vib-hspR401-422	GCVATGATHARHAGHGRRRCGNG		

### 3.2.4 Sequencing and Identification

Sequencing was performed through Eurofins Genomics (Louisville, KY) on cleaned PCR products by mixing 4 µL of either forward or reverse primer (5 pmol/µL) and 8 µL of the cleaned PCR product into a sequencing tube. Both forward and reverse sequences were obtained.

Forward and reverse sequences were analyzed through SnapGene Viewer for the quality of the sequence (Figure 14). The reverse complement of the reverse sequence was obtained for alignment purposes using SnapGene Viewer. The forward and reverse sequences were aligned

via Clustal Omega tool in EMBL-EBI (Maderia et al., 2022). Once the aligned sequences are obtained, the sequence is input into Nucleotide BLAST (Altschul et al., 1990) to search against the NCBI database for the identification of the bacterial species. A neighbor-joining phylogenetic tree was obtained through Clustal Omega in EMBL-EBI (Maderia et al., 2022).

### **3.2.3 Agar Recipe**

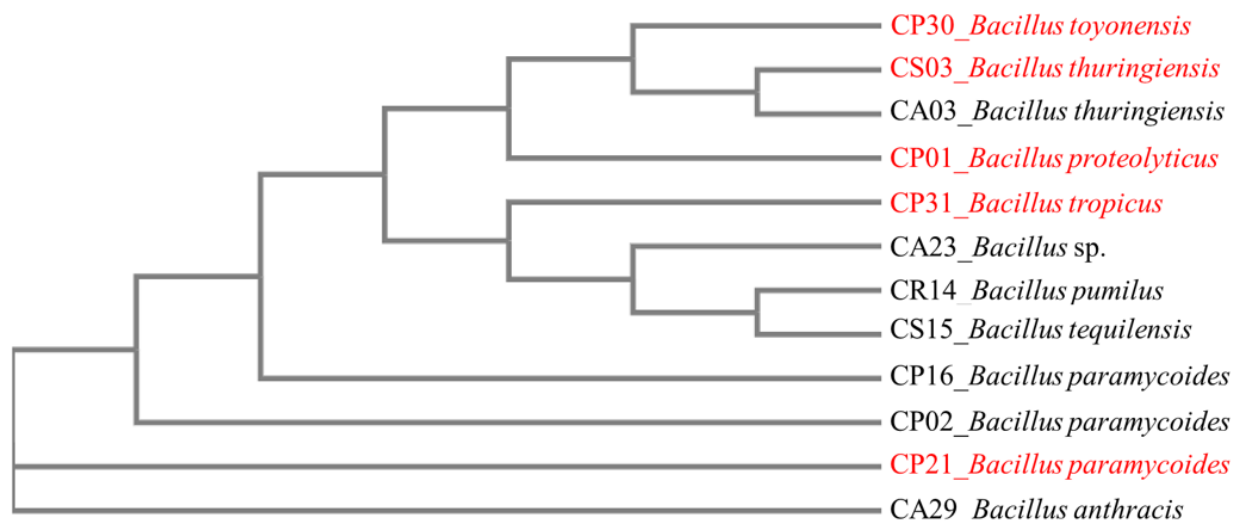
A1 agar was prepared by adding 10 g agar, 5 g starch, 2 g yeast, and 1 g peptone into a 1-L media bottle. In a flask, 600 mL of milli-Q was mixed with 15 g Instant Ocean and vacuum-filtered. The filtered salt water was then added to the 1-L media bottle and autoclaved for 30 minutes. Once the autoclave was done and the media bottle was cool enough to touch but still warm, the agar was poured into sterile Petri dishes in a Purifier Logic+ Class II, Type A2 Biosafety Cabinet (Labconco). TCBS agar (BD Difco™) was prepared based on the manufacturer's protocol. MC agar (ThermoFisher) was prepared based on the manufacturer's protocol with the addition of Instant Ocean (20 g/L).

## **3.3 Results and Discussion**

### **3.3.1 Identified Bacterial Strains**

The goal of this study was to identify the isolated, culturable bacterial strains that settled on the surface of *Caulerpa* spp. to understand the chemical mediation in the recruitment of certain bacteria. Out of 35 bacterial strains isolated from *Caulerpa* spp., 12 bacterial strains were identified via sequencing the 16S rRNA gene. The sequences of the identified bacterial strains were aligned and a neighbor-joining phylogenetic tree was obtained via Clustal Omega (Figure 11) (Madeira et al., 2022). A neighbor-joining tree is created by grouping similar (neighboring) sequences to minimize the total branch length, resulting in a minimum-evolution tree (Saitou & Nei, 1987). The phylogenetic tree was used to observe the diversity and types of bacteria

identified that were isolated from the surface of *Caulerpa* spp.. Bacterial strains labeled in red grew on TCBS agar plates, indicating that they are *Vibrio* spp. contrary to their 16S rRNA sequence identification. Bacterial strains labeled in black have shown no growth on TCBS agar plates, indicating they are not *Vibrio* spp.. Identification of environmental bacterial strains was proved to be quite challenging with many adjustments made in optimize each step.

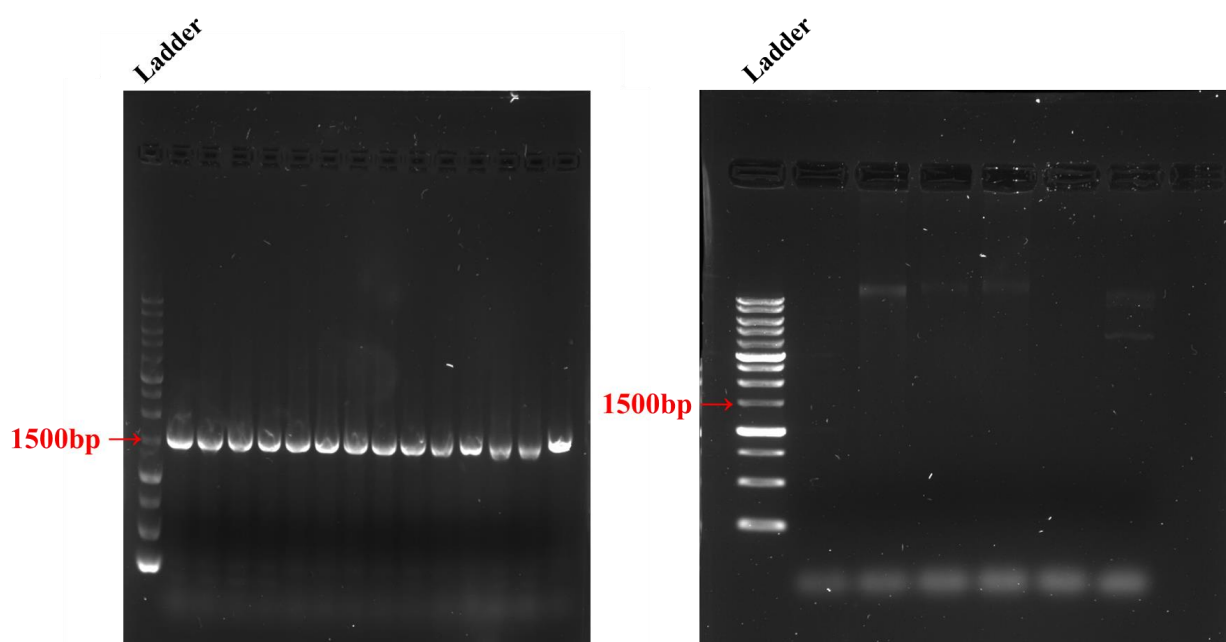


**Figure 11.** Phylogenetic tree of identified bacterial strains. For this study, a phylogenetic tree was used to distinguish different bacterial strains to observe the types of bacteria present. Code names of the bacterial strains are labeled as ‘C\_##’. Bacterial strains in red indicate growth on TCBS agar plates and the bacterial strains should be *Vibrio* spp. Bacterial strains in black indicate no growth on TCBS agar plates.

### 3.3.2 PCR Troubleshooting

The amplification of the 16S rRNA gene resulted in a 1,500 bp segment that can be viewed in a PCR gel. Figure 12 displays PCR gels in which the left gel was a successful PCR run and the right gel was an unsuccessful PCR run. The samples were compared to a 1 kb DNA ladder that was loaded into the first lane of the gel. A successful PCR run is indicated by a single bright, clear band at 1,500 bp (Figure 12, left gel). An unsuccessful PCR run is indicated

by no bands at 1,500 bp (Figure 12, right gel). All of the samples tested ran through the gel resulting in faint lines at the bottom of the gel, past the smallest band in the ladder. If the PCR run was unsuccessful, the PCR protocol and the quality of the DNA are re-evaluated.

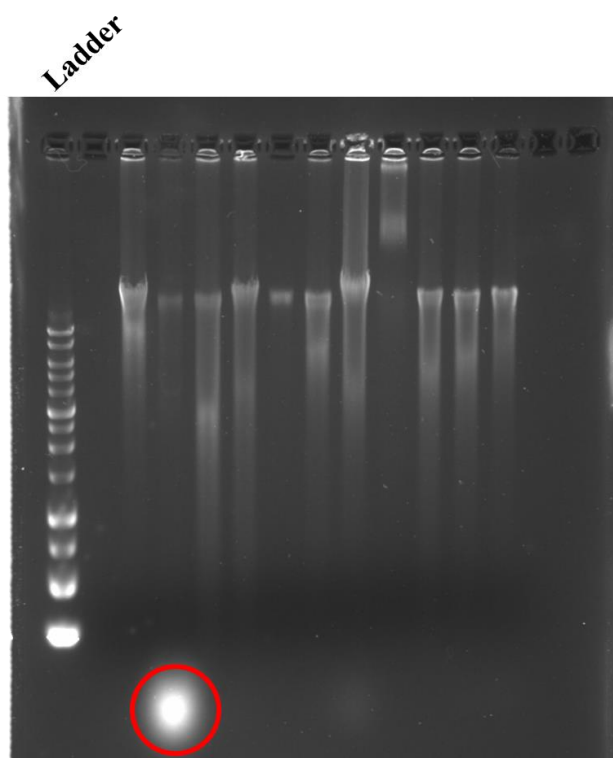


*Figure 12.* PCR gel for the amplification of the 16S rRNA gene. Left image indicates PCR worked and the PCR products are of the correct bp length (1,500 bp indicated in red). Right image indicates PCR did not work, indicated by the bands running to the bottom of the gel, past the smallest band in the ladder.

The PCR protocol and reagent ratios were adjusted various times in effort to optimize the PCR step in bacterial identification. For example, the annealing temperature was modified between 50-55°C to find the optimum temperature for the primers. The annealing temperature was initially determined to be 55°C because it is 5°C below the melting temperature of the primers.

The next speculation in effort to optimize PCR was to test the quality of the genomic DNA by running a genomic DNA gel (Figure 13). This process was similar to running a PCR

gel with the change of 5  $\mu$ L of genomic DNA rather than 5  $\mu$ L of PCR mixture with the same gel electrophoresis parameters. If the quality of the genomic DNA is good, the band would be visualized near the top of the gel due to its large bp size. However, if the genomic DNA has degraded, the band will run through the gel and past the smallest bp size compared to the ladder (Figure 13, red circle). If the genomic DNA degraded, then DNA extraction of that bacterial strain must be performed again. Re-evaluation of the DNA extraction step included the use of different liquid media for the optimal growth of these environmental bacterial strains. Each environmental bacterial strain may have unique media requirements.


















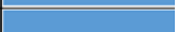



















*Figure 13.* Genomic DNA gel was used as quality control of the DNA extraction step to ensure the genomic DNA did not degrade for future steps. Genomic DNA should show a band relatively high in the gel due to its high molecular weight. The band circled in red indicates genomic DNA that has degraded because it passed through the gel farther than the smallest band in the ladder.

The degradation of genomic DNA in this study was likely due to the repeated freezing and thawing of the genomic DNA. Genomic DNA samples were found to degrade with an increase in freeze/thaw cycles and were directly related to the size of the DNA, i.e., the larger the DNA the more susceptible it was to degradation (Shao et al., 2012). In solution (e.g., water or buffer) DNA is a random coil, and when it freezes and thaws, ice crystals form causing tension leading to DNA breakage (Shao et al., 2012; Matange et al., 2021). With repeated freezing and thawing, the integrity of the DNA decreased exponentially (Matange et al., 2021). To solve this problem, aliquots of the genomic DNA extract should be made in order to keep the majority of extracted genomic DNA frozen until needed for PCR.




Another major issue in this process was the loss of PCR product after PCR cleanup was performed. The progress of each bacterial strain is listed in Table 2, with the progress of the DNA on the far right column. One reason may be that the volume of PCR mixture added to the column is too little and very little purified PCR product elutes off. In the manufacturer's protocol, up to 800  $\mu$ L of the PCR mixture and Binding Buffer are added to the column. However, the maximum volume used for one bacterial strain was 405  $\mu$ L (triplicate of one bacterial strain) that was added to the column. Most of the time, only a single or duplicate of a bacterial strain was used for PCR and, if successful, PCR cleanup. In most cases, the use of triplicates for PCR and PCR cleanup did result in high enough DNA concentrations for sequencing. Some purified PCR products had a DNA concentration right below the DNA concentration requirement for sequencing. In this case, double the amount of purified PCR products was added to the sequencing tube. This often resulted in low quality sequencing results (Figure 14, bottom), but some resulted in high quality sequencing results (Figure 14, top).

Table 3

*Progress of Identification of 35 Isolated Bacterial Strains from the Surface of Caulerpa spp.*

Bacterial Strain	Number of Times Sent for Sequencing	Number of Times Sequencing Failed	Progress
CS15	3	2	
CP16	2	1	
CA33	5	4	
CA03	4	3	
CP30	2	2	
CS16	3	2	
CP08	4	3	
CP04	4	3	
CA08	3	3	
CP19	-	-	
CP31	2	1	
CA14	7	7	
CP20	-	-	
CP18	5	4	
CP01	2	2	
CA23	2	0	
CP02	2	0	
CA15	2	1	
CR14	2	0	
CA09	4	3	
CP07	2	2	
CR01	6	6	
CS02	4	3	
CA18	-	-	
CP21	2	0	
CA31	10	9	
CA29	2	0	
CA02	2	2	
CA05	3	2	
CP27	7	7	
CP33	2	2	
CS03	2	0	
CS07	6	5	
CS09	6	6	
CP25	3	3	

**Key**

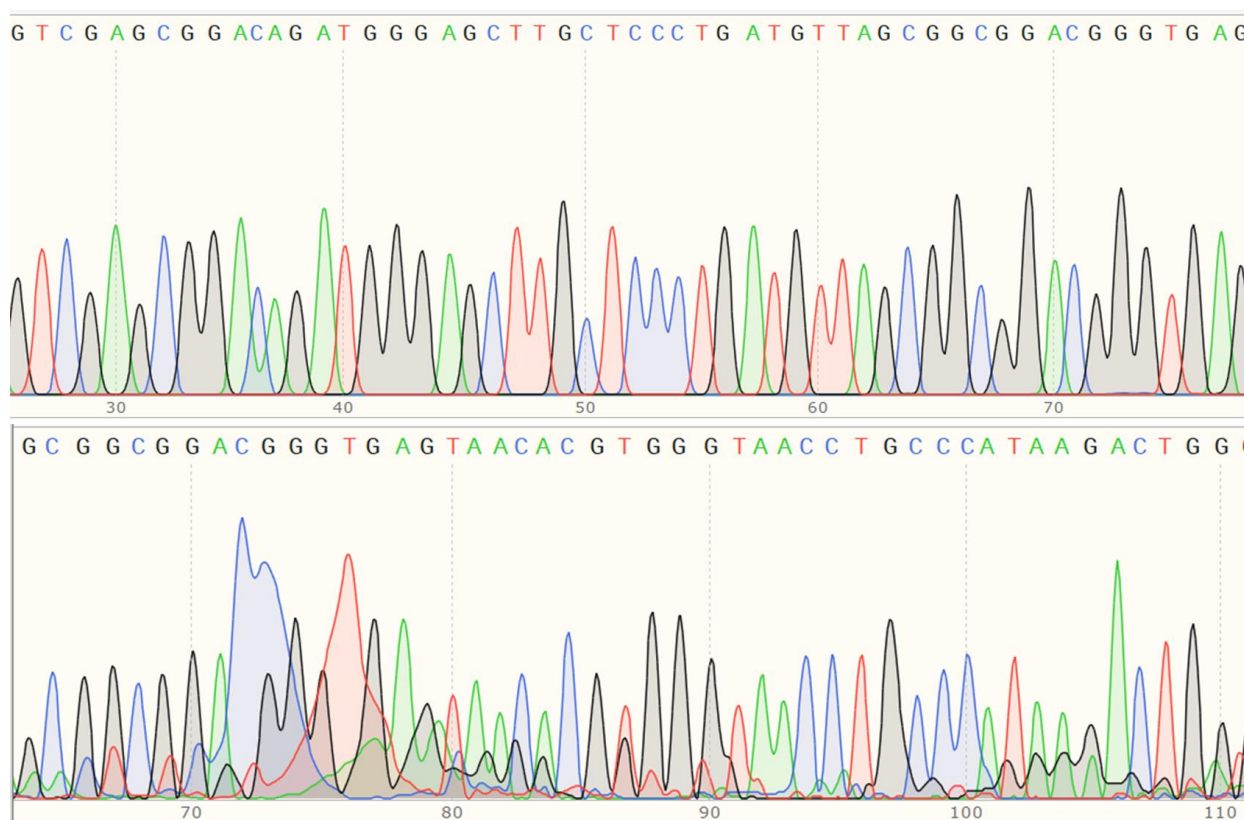
	Identified
	PCR Product
	Lost following PCR Cleanup

### 3.3.3 Sequencing and Identification

Sequencing of the bacterial strains included the combination of the forward and reverse sequence. The sequencing results are viewed and analyzed as a chromatogram in which each nucleotide is labeled with a color and indicated as a peak for detection (Figure 14). The forward and reverse sequencing results are analyzed and if both are high quality, the reverse complement of the reverse sequence was used, and they are aligned to achieve an almost 1,500 bp length sequence. However, if either the forward or reverse sequence was low quality only half of the full 16S rRNA sequence was obtained. A low quality sequence may be due to the bacterial strain containing multiple copies of the 16S rRNA gene and the copies have different sequences that all show up on the chromatogram (Patel, 2001). Partial sequencing of the forward sequence may be sufficient, but for accuracy of bacterial identification it was not enough, and the full 16S rRNA sequence is required (Patel, 2001). In many studies the 16S rRNA gene was partially sequenced of about 700 bp or shorter due to cost restraints with Sanger sequencing (Kim et al., 2011).

Rather than using the same primers that were used for PCR (27F and 1492R), which target all nine hypervariable regions, primers that target the middle hypervariable regions may result in better sequencing results. On the bottom of Figure 10, the primers used to attach to the 16S rRNA gene are aligned to the base they attach to. Therefore, primers such as 530F and 1100R should be used in the future to sequence a shorter region for better sequencing efficiency and results.



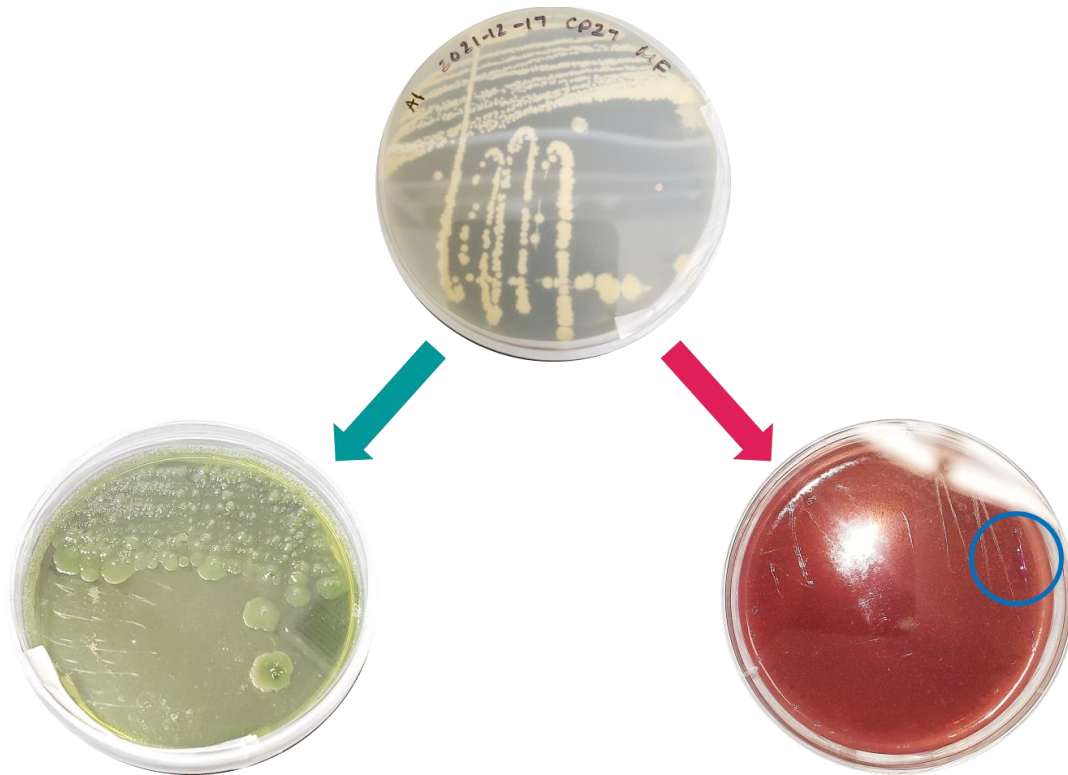


**Figure 14.** Sequencing results of the 16S rRNA gene. Top chromatogram depicts a high quality sequence in which all the bases are clearly identified based on the colored peaks. Bottom chromatogram depicts a low quality sequence in which the sequence cannot be read clearly, resulting in the detection of multiple bases.

### 3.3.4 Identification of *Vibrio* spp.

The identification of bacterial strains suspected to be *Vibrio* spp. according to agar studies resulted in *Bacillus* spp. (Figure 11). It is highly suspected that there is contamination by *Bacillus* endospores and the contaminant was sequenced and identified. All of the isolated bacterial strains were plated on A1 agar plates and TCBS agar plates for the detection of *Vibrio* spp. (Figure 15). The bacterial strains that grew on TCBS agar plates matched that of preliminary data. Based on these results, it was expected that these strains would be identified as *Vibrio* spp. when sequencing the 16S rRNA gene based on previous studies (Gomez-Gil et al., 2004; Thompson et al., 2005; Pascual et al., 2010).

Morphologically, some *Vibrio* spp. look very similar on TCBS agar plates and therefore require sequencing for identification or other identification assays (e.g., biochemical assays). In this study, MC agar was used to confirm *Vibrio* spp. (Figure 15). If growth was seen on TCBS agar, the bacterial strain, from A1 agar, was then plated on MC agar. Growth on MC agar plates was small but resulted in a pink-purple color on the initial streak. MC agar was used because it is both a differential and selective media for the growth of Gram-negative bacteria. Crystal violet (0.001 g/L) and bile salts (1.5 g/L) present in MC agar inhibits the growth of Gram-positive bacteria (Jung & Hoilat, 2021). If there was growth on both TCBS and MC, the bacterial strain was considered to be a *Vibrio* spp.. The 12 bacterial strains that are suspected *Vibrio* spp. were able to grow on both TCBS and MC agar (Table 3). However, some *Bacillus* spp. have the ability to withstand the crystal violet and bile salts present in MC agar. Thus, agar studies is not sufficient to confirm a bacterial strain is *Vibrio* spp. and suggests that *Bacillus* spp. contaminants were cultured and identified. Another method to classify the bacterial strains as Gram-positive or -negative is gram staining. *Vibrio* spp. are Gram-negative bacteria, which will result in a purple stain, and *Bacillus* spp. are Gram-positive bacteria, which will result in a red/pink stain. This simple method may provide rapid results for the classification of the bacteria present in the suspected *Vibrio* spp. stock cultures.



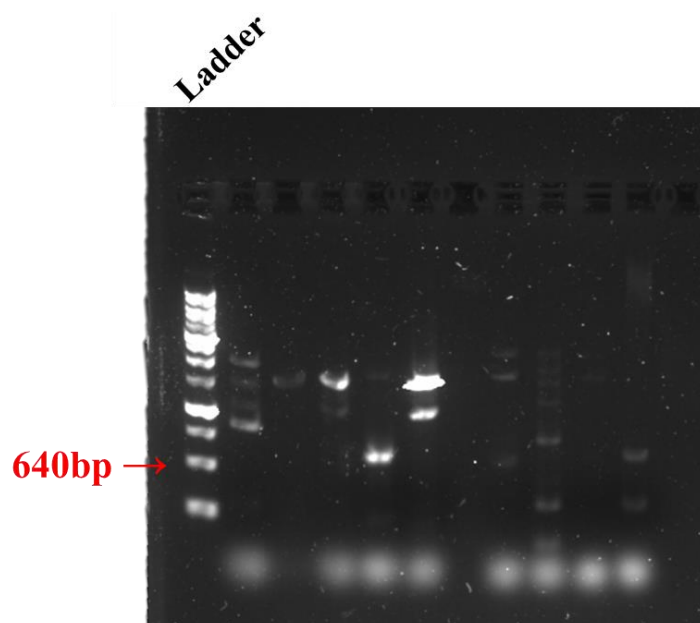
*Figure 15.* Agar plates to identify *Vibrio* spp. based on morphology. If growth was seen on TCBS agar, the bacterial strain, from A1 agar, was then plated on MC agar. Top agar plate is an A1 agar plate of a bacterial strain that is suspected to be a *Vibrio* spp.. Bottom left agar plate is a TCBS agar plate with growth, indicating the bacterial strain is a *Vibrio* spp.. Bottom right agar plate is a MC agar plate with little growth (circled in blue), further confirming the bacterial strain is a *Vibrio* spp..

Table 4  
*Growth of Vibrio spp. on TCBS and MC Agar*

<b>Suspected <i>Vibrio</i> spp.</b>	<b>TCBS</b>	<b>MC</b>
CP30	✓	✓
CP08	✓	✓
CA08	✓	✓
CP19	✓	✓
CP31	✓	✓
CP01	✓	✓
CA15	✓	✓
CS02	✓	✓
CP21	✓	✓
CP27	✓	✓
CS03	✓	✓
CS09	✓	✓

The use of vibrio-specific primers was the next consideration for sequence identification. There are a wide variety of primers for the identification of species-specific *Vibrio* spp. because there is not a single gene that can differentiate all *Vibrio* spp. (Thompson et al., 2005; Pascual et al., 2010). The identification of *Vibrio* spp. through the 16S rRNA gene was found to not be species-specific within the genus (Gomez-Gil et al., 2004). The *toxR* and *hsp60* genes were utilized for the genomic identification of *Vibrio* spp..

The *toxR* gene was selected because of its central role in transcriptional regulation of multiple virulence determinants which seems to be conserved within the family Vibrionaceae (V. Miller et al., 1987; Bauer & Rørvik, 2007). PCR was run to amplify the *toxR* gene using primers specific in Table 1. The PCR product size was expected to be 640 bp. The PCR run resulted in either various band sizes that did not match the expected or no amplification at all with the exception of one bacterial strain (Figure 16). However, there was no positive control used and it is uncertain if the PCR was successful in the amplification of the *toxR* gene. A known *Vibrio* spp. is needed as a positive control for the amplification of the *toxR* gene.



*Figure 16.* PCR gel for the amplification of the *toxR* gene. Only one bacterial strain showed a successful amplification of the *toxR* gene with the vibrio-specific primers used. All other bacterial strains showed multiple bands or no amplification.

The *hsp60* gene was then selected based on a previous study that demonstrated the *hsp60* gene could be used as a universal target for the identification of marine vibrios (Kwok et al., 2002). The *hsp60* gene, also known as *groEL*, is a chaperonin that mediates the folding of proteins and was shown to be a reliable gene for the identification and differentiation of *Vibrio* spp. (Brinker et al., 2001; Silvester et al., 2017). PCR was run to amplify the *hsp60* gene using primers specified in Table 1. The PCR product size was expected to be 420 bp. The PCR run resulted in various band sizes and no single band at 420 bp was seen (Figure 17). Additionally, there was no positive control used and the results of the PCR are uncertain, although most likely unsuccessful. A known *Vibrio* spp. is needed as a positive control for the amplification of the *hsp60* gene.

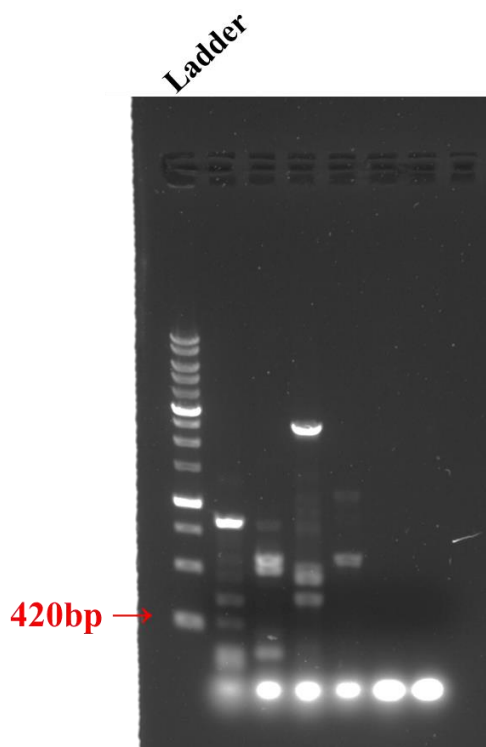


Figure 17. PCR gel for the amplification of the *hsp60* gene. Bacterial strains tested showed multiple bands. No bacterial strains were detected at 420 bp using vibrio-specific primers.

### 3.4 Summary

The identification of settled bacterial strains from the surface of *Caulerpa* spp. resulted in 12 identified bacterial strains through sequencing the 16S rRNA gene. Within these 12 identified bacterial strains, five bacterial strains are suspected to be *Vibrio* spp. based on their morphology on TCBS agar and MC agar plates. Various troubleshooting methods were performed in effort to optimize each step of the identification process before identifying the other 23 bacterial strains. *Vibrio*-specific primers were used to attempt to identify *Vibrio* spp. due to their identification as *Bacillus* spp. when the 16S rRNA gene was amplified and sequenced. Further assessment of these environmental bacterial strains are needed to optimize the process of bacterial identification for the other 23 bacterial strains.

## CHAPTER 4: PROTECTIVE BACTERIAL COMMUNITY ASSOCIATED WITH *MICROCHLOROPSIS SALINA*

Below is the original introduction for Fisher, C. L., Fong, M. V., Lane, P. D., Carlson, S., & Lane, T. W. (2022). *Cryo-storage and algal association of protective bacteria that protect *Microchloropsis salina* from grazing by *Brachionus plicatilis** [Communication submitted for publication July 28, 2022].

Materials and Methods, Results and Discussion can be found in the publication cited above. I performed data analysis, drawing conclusions, writing, and created figures which is included in the publication. The data in this study is not my work – data was collected by Lawrence Livermore National Laboratory.

### **4.1 Background**

The microalgal microbiome, which is the bacterial community associated with microalgae, are ubiquitous in algal cultures but has been often overlooked, therefore making it understudied compared to the volume of microalgae studies currently in the literature. There are more than 10 times the number of papers published, found on PubMed, on microalgae than that of the microalgal microbiome between the years 2010-2021. Interactions between microalgae and their associated microbes directly affect density, metabolism, and physiology (Yao et al., 2019; H. Wang et al., 2014), simultaneously participating individually in many symbioses – mutualism, commensalism, and parasitism (Ramanan et al., 2016; Molina et al., 2019; Fuentes et al., 2016). Co-cultivation of microalgae and ‘beneficial’ bacteria has been reported to enhance microalgae growth rate by up to 10% thereby increasing biomass production (Ramanan et al.,

2016). However, these growth promoting bacterial communities have not been characterized to a genus or species level. Bacteria play an important role providing nutrients (e.g., carbon, nitrogen, phosphorus, sulfur, iron, etc.) essential for algal growth (Hannon et al., 2010; Amin et al., 2012; Buchan et al., 2014; Lian et al., 2018). In a survey of 326 algal species, over half were dependent on bacteria as an external source for vitamin B12 for growth (Croft et al., 2005), signifying the importance of algal-bacteria interactions. Thus, bacteria play a critical role in the growth and survival of microalgae and require further study.

The presence of bacteria is ubiquitous in microalgal production systems. Microalgae begin in closed photobioreactors and then are mass cultivated in open pond systems. Open pond systems, also known as raceway systems, operate using a paddle wheel to circulate algae in parallel channels (Zittelli et al., 2013). These are the most common commercial systems to produce algal biofuels due to the lower cost relative to closed reactors (Zittelli et al., 2013; Hannon et al., 2010). Open algal ponds, however, are more susceptible to crashing, often resulting in a total loss of an algal crop. Closed photobioreactors contain the microalgae culture within a transparent vessel restricting the interactions between the culture and contaminants from the surrounding environment and potentially maintaining axenic cultures (Zittelli et al., 2013). While closed photobioreactors have a lower probability of contamination, once contaminated, they are difficult and expensive to clean and decontaminate (B. Wang et al., 2012; Kazamia et al., 2014). Pond crashes are caused by a number of factors, such as contamination from other algae species or unwanted pests such as viruses, fungi, protozoans, and harmful bacteria (Hannon et al., 2010; Lam et al., 2018). Current industrial routines to mitigate and treat pond crashes fall into one of two categories: physical (e.g., filtration, sonication, and environmental modifications) or chemical methods (e.g., antibiotics, pesticides, high salinity, high alkalinity, aldehydes, and



peroxides) (Molina et al., 2019; Zhu et al., 2020). These strategies are costly and time-consuming and may cause deleterious environment impacts. Moreover, they are not guaranteed to succeed, especially on an industrial scale, and resistance to pesticides is a common result that renders these types of treatment ineffective over long periods of time (McBride et al., 2014). Previous studies have suggested the use of bacteria as a type of built-in biocontrol to inhibit pests from causing algal pond crashes (Fisher et al., 2019; Natrah et al., 2011; Kazamia et al., 2014). Deines et al. demonstrated rotifer and other pest survival can be decreased to extinction within a culture by violacein-producing bacteria within two days (Deines et al., 2009). Therefore, it remains necessary to continue to develop new strategies to prevent pond crashes, improve microalgae cultivation, and bring commercially available algal biofuels to commercial market.

Microalgae biomass can be converted into biofuels through three subclasses of conversions – chemical, biochemical, and thermochemical conversions which can be used as an alternative energy source to replace fossil fuels (Milano et al., 2016). Fossil fuels are nonrenewable energy sources that have been used for centuries. The release of carbon dioxide (CO<sub>2</sub>) and other greenhouse gases from fossil fuels has contributed to global warming and climate change. While biofuels have been proposed as an energy alternative (Khan et al., 2018) there are many challenges to overcome. First-generation biofuels were produced from edible crops such as maize, sugarcane, and wheat (R. Lee & Lavoie, 2013). Second-generation biofuels are produced from the non-edible portions of crops called lignocellulose (R. Lee & Lavoie, 2013). First- and second-generation biofuels are dependent on cultivable land and compete with crops grown for human consumption (Alishah Aratboni et al., 2019). Third generation biofuels, produced by microalgae, have recently gained in popularity due to their clear advantages over first- and second-generation biofuels. Microalgae grow much faster than first- and second-

generation crops on smaller acreage unsuitable for agriculture. Under the right conditions, microalgae double their biomass within 24 hours, potentially producing a higher oil yield than crops (Chisti, 2007; Hannon et al., 2010). Microalgae use CO<sub>2</sub> as a feedstock from various sources, such as the atmosphere and exhaust gases from industrial practices to produce biofuels (B. Wang et al., 2008). Current limitations to algal biofuels include strain development for maximizing lipid content, nutrient circulation and light exposure throughout a culture, and higher energy input compared to terrestrial energy crops (Hannon et al., 2010; Lam & Lee, 2012). The marine microalga utilized in this study, *Microchloropsis salina*, is a promising candidate for biofuel production due to algae's production of large quantities of lipids, yielding an oil content of 31-68% by dry weight (Medipally et al., 2015; Chisti, 2007).

In this study, we investigated the marine microalga *Microchloropsis salina* and the effect of different bacterial communities added to *M. salina* cultures in the presence and absence of the marine rotifer *Brachionus plicatilis*. *B. plicatilis*, a common contaminant in algal ponds, ingests 200 microalgal cells per minute, resulting in significant loss of an algal crop and diminishing algal biofuel production (Hirayama & Ogawa, 1972; Molina et al., 2019). These cultures, both in the presence and absence of rotifers, were size-filtered through 41ret, 0.8ret, and 0.22ret fractions to identify bacteria associated with *B. plicatilis*, *M. salina*, and those in an unassociated lifecycle, respectively. The bacterial communities of each filtered set were sequenced and classified into individual operational taxonomic units (OTUs). Certain OTUs were observed to have a protective effect on the microalgal culture in the presence of *B. plicatilis* by allowing the microalgae to survive in conjunction with rotifers. Our aim is to identify protective bacteria present in the presence of *B. plicatilis* that are absent in the absence of *B. plicatilis* in order to

devise a biocontrol to mitigate pest contamination without the use of current, flawed industrial decontamination strategies.

## 4.2 Summary

Based on these data, we show key taxa in the added protective bacterial communities that prevented grazing by *B. plicatilis*. This study shows the difference in bacterial composition of the bacterial communities in the presence and absence of *B. plicatilis* while showing specific bacteria associated with *B. plicatilis*, *M. salina*, and those unassociated. This data supports the novel use of bacteria as a cost-effective bio-control method to mitigate contamination by rotifers for the enhancement of microalgae biofuels. Future studies will continue to investigate bacteria in these protective bacterial communities and its chemical mechanisms.

## CHAPTER 5: SUMMARY AND FUTURE DIRECTIONS

This work provides examples of the role natural products play in bacterial communication. In chapter 2, a GLP was partially characterized in both VP EPS and V+S crude extracts through LC-MS/MS. The GLP is not responsible for *S. aureus* biofilm inhibition, therefore fractions of VP EPS, VP Mut 35, V+S, and 35+S crude extracts are being tested for their biofilm inhibition activity. Further separation and isolation of the bioactive molecule is needed to elucidate the structure of the biofilm inhibitor. Of the 35 bacterial isolates from the surface of *Caulerpa* spp., 12 were identified as *Bacillus* spp. through sequencing the 16S rRNA gene in chapter 3. Further optimization for the identification of *Vibrio* spp. is needed to support our hypothesis that *Caulerpa* spp. chemically mediates its surface microbiome by recruiting a higher percentage of *Vibrio* spp.. Chapter 4 compared the composition of bacterial communities in the presence and absence of *B. plicatilis* indicates that some genera of bacteria that are microalgae-, rotifer-associated, or free-floating may play a role in protecting *M. salina* from grazing by rotifers. The chemistry involved between the protective bacterial community and *M. salina* is needed to enhance microalgal biofuel production. Bacteria and their metabolites play an important role through their interactions in microbial communities and with other organisms. The identification of bacteria and their metabolites key to understanding and characterizing these observed interactions.

## REFERENCES

- Aires, T., Moalic, Y., Serrao, E. A., & Arnaud-Haond, S. (2015). Hologenome theory supported by cooccurrence networks of species-specific bacterial communities in siphonous algae (Caulerpa). *FEMS Microbiology Ecology*, 91(7). <https://doi.org/10.1093/femsec/fiv067>
- Alishah Aratboni, H., Rafiei, N., Garcia-Granados, R., Alemzadeh, A., & Morones-Ramírez, J. R. (2019). Biomass and lipid induction strategies in microalgae for biofuel production and other applications. *Microbial Cell Factories*, 18(1), 178. <https://doi.org/10.1186/s12934-019-1228-4>
- Altschul, S. F., Gish, W., Miller, W., Myers, E. W., & Lipman, D. J. (1990). Basic local alignment search tool. *Journal of Molecular Biology*, 215(3), 403–410. [https://doi.org/10.1016/S0022-2836\(05\)80360-2](https://doi.org/10.1016/S0022-2836(05)80360-2)
- Amin, S. A., Parker, M. S., & Armbrust, E. V. (2012). Interactions between diatoms and bacteria. *Microbiology and Molecular Biology Reviews: MMBR*, 76(3), 667–684. <https://doi.org/10.1128/MMBR.00007-12>
- Arnaud-Haond, S., Aires, T., Candeias, R., Teixeira, S. J. L., Duarte, C. M., Valero, M., & Serrão, E. A. (2017). Entangled fates of holobiont genomes during invasion: nested bacterial and host diversities in *Caulerpa taxifolia*. *Molecular Ecology*, 26(8), 2379–2391. <https://doi.org/10.1111/mec.14030>
- Atanasov, A. G., Zotchev, S. B., Dirsch, V. M., International Natural Product Sciences Taskforce, & Supuran, C. T. (2021). Natural products in drug discovery: advances and opportunities. *Nature Reviews. Drug Discovery*, 20(3), 200–216. <https://doi.org/10.1038/s41573-020-00114-z>

- Baker-Austin, C., Oliver, J. D., Alam, M., Ali, A., Waldor, M. K., Qadri, F., & Martinez-Urtaza, J. (2018). *Vibrio* spp. infections. *Nature Reviews. Disease Primers*, 4(1), 8.  
<https://doi.org/10.1038/s41572-018-0005-8>
- Banat, I. M., De Rienzo, M. A. D., & Quinn, G. A. (2014). Microbial biofilms: biosurfactants as antibiofilm agents. *Applied Microbiology and Biotechnology*, 98(24), 9915–9929.  
<https://doi.org/10.1007/s00253-014-6169-6>
- Bauer, A., & Rørvik, L. M. (2007). A novel multiplex PCR for the identification of *Vibrio parahaemolyticus*, *Vibrio cholerae* and *Vibrio vulnificus*. *Letters in Applied Microbiology*, 45(4), 371–375. <https://doi.org/10.1111/j.1472-765X.2007.02195.x>
- Blin, K., Shaw, S., Kloosterman, A. M., Charlop-Powers, Z., van Wezel, G. P., Medema, M. H., & Weber, T. (2021). antiSMASH 6.0: improving cluster detection and comparison capabilities. *Nucleic Acids Research*, 49(W1), W29–W35.  
<https://doi.org/10.1093/nar/gkab335>
- Boddy, C. N. (2014). Bioinformatics tools for genome mining of polyketide and non-ribosomal peptides. *Journal of Industrial Microbiology & Biotechnology*, 41(2), 443–450.  
<https://doi.org/10.1007/s10295-013-1368-1>
- Brennan-Krohn, T., Pica, N., Sandora, T. J., & McAdam, A. (2016). The Brief Case: Safe To Go Back in the Water? *Vibrio parahaemolyticus* Wound Infection Associated with Brackish Water. *Journal of Clinical Microbiology*, 54(6), 1414–1415.  
<https://doi.org/10.1128/JCM.02660-15>
- Brinker, A., Pfeifer, G., Kerner, M. J., Naylor, D. J., Hartl, F. U., & Hayer-Hartl, M. (2001). Dual function of protein confinement in chaperonin-assisted protein folding. *Cell*, 107(2), 223–233. [https://doi.org/10.1016/s0092-8674\(01\)00517-7](https://doi.org/10.1016/s0092-8674(01)00517-7)

- Buchan, A., LeClerc, G. R., Gulvik, C. A., & González, J. M. (2014). Master recyclers: features and functions of bacteria associated with phytoplankton blooms. *Nature Reviews. Microbiology*, 12(10), 686–698. <https://doi.org/10.1038/nrmicro3326>
- Camilli, A., & Bassler, B. L. (2006). Bacterial small-molecule signaling pathways. *Science*, 311(5764), 1113–1116. <https://doi.org/10.1126/science.1121357>
- Capone, D. G., Zehr, J. P., Paerl, H. W., Bergman, B., & Carpenter, E. J. (1997). *Trichodesmium*, a Globally Significant Marine Cyanobacterium. *Science*, 276(5316), 1221–1229. <https://doi.org/10.1126/science.276.5316.1221>
- Carroll, A. R., Copp, B. R., Davis, R. A., Keyzers, R. A., & Prinsep, M. R. (2020). Marine natural products. *Natural Product Reports*, 37(2), 175–223. <https://doi.org/10.1039/c9np00069k>
- Chakravorty, S., Helb, D., Burday, M., Connell, N., & Alland, D. (2007). A detailed analysis of 16S ribosomal RNA gene segments for the diagnosis of pathogenic bacteria. *Journal of Microbiological Methods*, 69(2), 330–339. <https://doi.org/10.1016/j.mimet.2007.02.005>
- Chisti, Y. (2007). Biodiesel from microalgae. *Biotechnology Advances*, 25(3), 294–306. <https://doi.org/10.1016/j.biotechadv.2007.02.001>
- Croft, M. T., Lawrence, A. D., Raux-Deery, E., Warren, M. J., & Smith, A. G. (2005). Algae acquire vitamin B12 through a symbiotic relationship with bacteria. *Nature*, 438(7064), 90–93. <https://doi.org/10.1038/nature04056>
- Damodaran, S. E., & Madhan, S. (2011). Telavancin: A novel lipoglycopeptide antibiotic. *Journal of Pharmacology & Pharmacotherapeutics*, 2(2), 135–137. <https://doi.org/10.4103/0976-500X.81918>

- Daniel-Ivad, M., Pimentel-Elardo, S., & Nodwell, J. R. (2018). Control of Specialized Metabolism by Signaling and Transcriptional Regulation: Opportunities for New Platforms for Drug Discovery? *Annual Review of Microbiology*, 72, 25–48.  
<https://doi.org/10.1146/annurev-micro-022618-042458>
- Das, B., Sarkar, C., Das, D., Gupta, A., Kalra, A., & Sahni, S. (2017). Telavancin: a novel semisynthetic lipoglycopeptide agent to counter the challenge of resistant Gram-positive pathogens. *Therapeutic Advances in Infectious Disease*, 4(2), 49–73.  
<https://doi.org/10.1177/2049936117690501>
- Davies, D. (2003). Understanding biofilm resistance to antibacterial agents. *Nature Reviews. Drug Discovery*, 2(2), 114–122. <https://doi.org/10.1038/nrd1008>
- De Simeis, D., & Serra, S. (2021). Actinomycetes: A Never-Ending Source of Bioactive Compounds-An Overview on Antibiotics Production. *Antibiotics (Basel, Switzerland)*, 10(5). <https://doi.org/10.3390/antibiotics10050483>
- Deines, P., Matz, C., & Jürgens, K. (2009). Toxicity of violacein-producing bacteria fed to bacterivorous freshwater plankton. *Limnology and Oceanography*, 54(4), 1343–1352.  
<https://doi.org/10.4319/lo.2009.54.4.1343>
- Del Pozo, J. L. (2018). Biofilm-related disease. *Expert Review of Anti-Infective Therapy*, 16(1), 51–65. <https://doi.org/10.1080/14787210.2018.1417036>
- Dias, D. A., Urban, S., & Roessner, U. (2012). A historical overview of natural products in drug discovery. *Metabolites*, 2(2), 303–336. <https://doi.org/10.3390/metabo2020303>
- Discovery and Development of Penicillin*. (n.d.). American Chemical Society. Retrieved 2 September 2022, from



<https://www.acs.org/content/acs/en/education/whatischemistry/landmarks/flemingpenicillin.html>

- Dobretsov, S., Dahms, H. U., Harder, T., & Qian, P. Y. (2006). Allelochemical defense against epibiosis in the macroalga *Caulerpa racemosa* var. *turbinata*. *Marine Ecology Progress Series*, 318, 165–175. <https://doi.org/10.3354/meps318165>
- Fischbach, M. A., & Walsh, C. T. (2006). Assembly-line enzymology for polyketide and nonribosomal Peptide antibiotics: logic, machinery, and mechanisms. *Chemical Reviews*, 106(8), 3468–3496. <https://doi.org/10.1021/cr0503097>
- Fisher, C. L., Fong, M. V., Lane, P. D., Carlson, S., & Lane, T. W. (2022). *Cryo-storage and algal association of protective bacteria that protect Microchloropsis salina from grazing by Brachionus plicatilis* [Communication submitted for publication July 28, 2022].
- Fisher, C. L., Ward, C. S., Lane, P. D., Kimbrel, J. A., Sale, K. L., Stuart, R. K., ... Lane, T. W. (2019). Bacterial communities protect the alga *Microchloropsis salina* from grazing by the rotifer *Brachionus plicatilis*. *Algal Research*, 40, 101500. <https://doi.org/10.1016/j.algal.2019.101500>
- Fleming, A. (1980). Classics in infectious diseases: on the antibacterial action of cultures of a penicillium, with special reference to their use in the isolation of B. influenzae by Alexander Fleming, Reprinted from the British Journal of Experimental Pathology 10:226-236, 1929. *Reviews of Infectious Diseases*, 2(1), 129–139. <https://www.ncbi.nlm.nih.gov/pubmed/6994200>
- Flemming, H.-C., Neu, T. R., & Wozniak, D. J. (2007). The EPS Matrix: The ‘House of Biofilm Cells’. *Journal of Bacteriology*, 189(22), 7945–7947. <https://doi.org/10.1128/JB.00858-07>

Flemming, H.-C., Wingender, J., Szewzyk, U., Steinberg, P., Rice, S. A., & Kjelleberg, S.

(2016). Biofilms: an emergent form of bacterial life. *Nature Reviews. Microbiology*, 14(9), 563–575. <https://doi.org/10.1038/nrmicro.2016.94>

Franco, A., Rückert, C., Blom, J., Busche, T., Reichert, J., Schubert, P., ... Glaeser, S. P. (2020).

High diversity of *Vibrio* spp. associated with different ecological niches in a marine aquaria system and description of *Vibrio aquimaris* sp. nov. *Systematic and Applied Microbiology*, 43(5), 126123. <https://doi.org/10.1016/j.syapm.2020.126123>

Fuentes, J. L., Garbayo, I., Cuaresma, M., Montero, Z., González-Del-Valle, M., & Vílchez, C.

(2016). Impact of Microalgae-Bacteria Interactions on the Production of Algal Biomass and Associated Compounds. *Marine Drugs*, 14(5), 100.

<https://doi.org/10.3390/md14050100>

Fukuda, K., Ogawa, M., Taniguchi, H., & Saito, M. (2016). Molecular Approaches to Studying

Microbial Communities: Targeting the 16S Ribosomal RNA Gene. *Journal of UOEH*, 38(3), 223–232. <https://doi.org/10.7888/juoeh.38.223>

Gaynes, R. (2017). The Discovery of Penicillin—New Insights After More Than 75 Years of

Clinical Use. *Emerging Infectious Diseases*, 23(5), 849.

<https://doi.org/10.3201/eid2305.161556>

Goecke, F., Labes, A., Wiese, J., & Imhoff, J. F. (2010). Chemical interactions between marine macroalgae and bacteria. *Marine Ecology Progress Series*, 409, 267–299.

<https://doi.org/10.3354/meps08607>

Gomez, E. (2022). *Inhibition of Staphylococcus aureus biofilm by Variovorax paradoxus*

[Master's thesis, University of the Pacific].

[https://scholarlycommons.pacific.edu/uop\\_etds/3803](https://scholarlycommons.pacific.edu/uop_etds/3803)

- Gomez-Gil, B., Soto-Rodríguez, S., García-Gasca, A., Roque, A., Vazquez-Juarez, R., Thompson, F. L., & Swings, J. (2004). Molecular identification of *Vibrio harveyi*-related isolates associated with diseased aquatic organisms. *Microbiology*, *150*(Pt 6), 1769–1777. <https://doi.org/10.1099/mic.0.26797-0>
- Han, J.-I., Choi, H.-K., Lee, S.-W., Orwin, P. M., Kim, J., Laroe, S. L., ... Han, C. (2011). Complete genome sequence of the metabolically versatile plant growth-promoting endophyte *Variovorax paradoxus* S110. *Journal of Bacteriology*, *193*(5), 1183–1190. <https://doi.org/10.1128/JB.00925-10>
- Hannon, M., Gimpel, J., Tran, M., Rasala, B., & Mayfield, S. (2010). Biofuels from algae: challenges and potential. *Biofuels*, *1*(5), 763–784. <https://doi.org/10.4155/bfs.10.44>
- Harvey, A. L., Edrada-Ebel, R., & Quinn, R. J. (2015). The re-emergence of natural products for drug discovery in the genomics era. *Nature Reviews. Drug Discovery*, *14*(2), 111–129. <https://doi.org/10.1038/nrd4510>
- Hay, M. E. (2009). Marine chemical ecology: chemical signals and cues structure marine populations, communities, and ecosystems. *Annual Review of Marine Science*, *1*, 193–212. <https://doi.org/10.1146/annurev.marine.010908.163708>
- Hirata, Y., & Uemura, D. (1986). Halichondrins - antitumor polyether macrolides from a marine sponge. *Journal of Macromolecular Science, Part A: Pure and Applied Chemistry*, *58*(5), 701–710. <https://doi.org/10.1351/pac198658050701>
- Hirayama, K., & Ogawa, S. (1972). Fundamental studies on physiology of rotifer for its mass culture – I: filter feeding of rotifer. *Bulletin of the Japanese Society of Scientific Fisheries*, *38*(11), 1207–1214. <https://doi.org/10.2331/suisan.38.1207>

- Hochbaum, A. I., Kolodkin-Gal, I., Foulston, L., Kolter, R., Aizenberg, J., & Losick, R. (2011). Inhibitory effects of D-amino acids on *Staphylococcus aureus* biofilm development. *Journal of Bacteriology*, 193(20), 5616–5622. <https://doi.org/10.1128/JB.05534-11>
- Hug, J. J., Krug, D., & Müller, R. (2020). Bacteria as genetically programmable producers of bioactive natural products. *Nature Reviews Chemistry*, 4(4), 172–193. <https://doi.org/10.1038/s41570-020-0176-1>
- Jain, A., & Tailor, V. (2020). Emerging Trends of Biotechnology in Marine Bioprospecting: A New Vision. In N. M. Nathani, C. Mootapally, I. R. Gadhvi, B. Maitreya, & C. G. Joshi (Eds.), *Marine Niche: Applications in Pharmaceutical Sciences : Translational Research* (pp. 1–36). Springer Singapore. [https://doi.org/10.1007/978-981-15-5017-1\\_1](https://doi.org/10.1007/978-981-15-5017-1_1)
- Johnston, C. W., Skinnider, M. A., Wyatt, M. A., Li, X., Ranieri, M. R. M., Yang, L., ... Magarvey, N. A. (2015). An automated Genomes-to-Natural Products platform (GNP) for the discovery of modular natural products. *Nature Communications*, 6, 8421. <https://doi.org/10.1038/ncomms9421>
- Jung, B., & Hoilat, G. J. (2021). MacConkey Medium. In *StatPearls*. StatPearls Publishing. <https://www.ncbi.nlm.nih.gov/books/NBK557394/>
- Kautsar, S. A., Blin, K., Shaw, S., Navarro-Muñoz, J. C., Terlouw, B. R., van der Hooft, J. J. J., ... Medema, M. H. (2020). MIBiG 2.0: a repository for biosynthetic gene clusters of known function. *Nucleic Acids Research*, 48(D1), D454–D458. <https://doi.org/10.1093/nar/gkz882>
- Kazamia, E., Riseley, A. S., Howe, C. J., & Smith, A. G. (2014). An Engineered Community Approach for Industrial Cultivation of Microalgae. *Industrial Biotechnology*, 10(3), 184–190. <https://doi.org/10.1089/ind.2013.0041>

- Kerr, R. G., Haltli, B. A., Marchbank, D. H., & Berru  , F. (2019). *Glycolipopeptide biosurfactants* (U.S. Patent No. 20190127411:A1). United States Patent and Trademark Office.  
<https://patentimages.storage.googleapis.com/eb/70/9a/635a04963e104f/US20190127411A1.pdf>
- Khan, M. I., Shin, J. H., & Kim, J. D. (2018). The promising future of microalgae: current status, challenges, and optimization of a sustainable and renewable industry for biofuels, feed, and other products. *Microbial Cell Factories*, 17(1), 36. <https://doi.org/10.1186/s12934-018-0879-x>
- Kim, M., Morrison, M., & Yu, Z. (2011). Evaluation of different partial 16S rRNA gene sequence regions for phylogenetic analysis of microbiomes. *Journal of Microbiological Methods*, 84(1), 81–87. <https://doi.org/10.1016/j.mimet.2010.10.020>
- King, W. L., Siboni, N., Kahlke, T., Green, T. J., Labbate, M., & Seymour, J. R. (2019). A New High Throughput Sequencing Assay for Characterizing the Diversity of Natural Vibrio Communities and Its Application to a Pacific Oyster Mortality Event. *Frontiers in Microbiology*, 10, 2907. <https://doi.org/10.3389/fmicb.2019.02907>
- Kolodkin-Gal, I., Romero, D., Cao, S., Clardy, J., Kolter, R., & Losick, R. (2010). D-amino acids trigger biofilm disassembly. *Science*, 328(5978), 627–629.  
<https://doi.org/10.1126/science.1188628>
- Kurth, C., Schieferdecker, S., Athanasopoulou, K., Seccareccia, I., & Nett, M. (2016). Variochelins, Lipopeptide Siderophores from Variovorax boronicumulans Discovered by Genome Mining. *Journal of Natural Products*, 79(4), 865–872.  
<https://doi.org/10.1021/acs.jnatprod.5b00932>

- Kwok, A. Y. C., Wilson, J. T., Coulthart, M., Ng, L.-K., Mutharia, L., & Chow, A. W. (2002). Phylogenetic study and identification of human pathogenic *Vibrio* species based on partial hsp60 gene sequences. *Canadian Journal of Microbiology*, 48(10), 903–910. <https://doi.org/10.1139/w02-089>
- Lam, M. K., & Lee, K. T. (2012). Microalgae biofuels: A critical review of issues, problems and the way forward. *Biotechnology Advances*, 30(3), 673–690. <https://doi.org/10.1016/j.biotechadv.2011.11.008>
- Lam, T. P., Lee, T.-M., Chen, C.-Y., & Chang, J.-S. (2018). Strategies to control biological contaminants during microalgal cultivation in open ponds. *Bioresource Technology*, 252, 180–187. <https://doi.org/10.1016/j.biortech.2017.12.088>
- Lee, M. D., Walworth, N. G., McParland, E. L., Fu, F.-X., Mincer, T. J., Levine, N. M., ... Webb, E. A. (2017). The *Trichodesmium* consortium: conserved heterotrophic co-occurrence and genomic signatures of potential interactions. *The ISME Journal*, 11(8), 1813–1824. <https://doi.org/10.1038/ismej.2017.49>
- Lee, R. A., & Lavoie, J.-M. (2013). From first- to third-generation biofuels: Challenges of producing a commodity from a biomass of increasing complexity. *Animal Frontiers*, 3(2), 6–11. <https://doi.org/10.2527/af.2013-0010>
- Letchumanan, V., Chan, K.-G., & Lee, L.-H. (2014). *Vibrio parahaemolyticus*: a review on the pathogenesis, prevalence, and advance molecular identification techniques. *Frontiers in Microbiology*, 5, 705. <https://doi.org/10.3389/fmicb.2014.00705>
- Lian, J., Wijffels, R. H., Smidt, H., & Sipkema, D. (2018). The effect of the algal microbiome on industrial production of microalgae. *Microbial Biotechnology*, 11(5), 806–818. <https://doi.org/10.1111/1751-7915.13296>

- Machado, H., Tuttle, R. N., & Jensen, P. R. (2017). Omics-based natural product discovery and the lexicon of genome mining. *Current Opinion in Microbiology*, 39, 136–142.  
<https://doi.org/10.1016/j.mib.2017.10.025>
- Madeira, F., Pearce, M., Tivey, A. R. N., Basutkar, P., Lee, J., Edbali, O., ... Lopez, R. (2022). Search and sequence analysis tools services from EMBL-EBI in 2022. *Nucleic Acids Research*, 50(W1), W276–W279. <https://doi.org/10.1093/nar/gkac240>
- Madhusoodanan, N. (2019, September 3). *Clustal Omega FAQ*. EMBL's European Bioinformatics Institute.  
<https://www.ebi.ac.uk/seqdb/confluence/display/JDSAT/Clustal+Omega+FAQ>
- Malabarba, A., & Goldstein, B. P. (2005). Origin, structure, and activity in vitro and in vivo of dalbavancin. *The Journal of Antimicrobial Chemotherapy*, 55 Suppl 2, ii15–ii20.  
<https://doi.org/10.1093/jac/dki005>
- Matange, K., Tuck, J. M., & Keung, A. J. (2021). DNA stability: a central design consideration for DNA data storage systems. *Nature Communications*, 12(1), 1358.  
<https://doi.org/10.1038/s41467-021-21587-5>
- McBride, R. C., Lopez, S., Meenach, C., Burnett, M., Lee, P. A., Nohilly, F., & Behnke, C. (2014). Contamination Management in Low Cost Open Algae Ponds for Biofuels Production. *Industrial Biotechnology*, 10(3), 221–227.  
<https://doi.org/10.1089/ind.2013.0036>
- McErlean, M., Overbay, J., & Van Lanen, S. (2019). Refining and expanding nonribosomal peptide synthetase function and mechanism. *Journal of Industrial Microbiology & Biotechnology*, 46(3-4), 493–513. <https://doi.org/10.1007/s10295-018-02130-w>

- Medema, M. H., Kottmann, R., Yilmaz, P., Cummings, M., Biggins, J. B., Blin, K., ... Glöckner, F. O. (2015). Minimum Information about a Biosynthetic Gene cluster. *Nature Chemical Biology*, 11(9), 625–631. <https://doi.org/10.1038/nchembio.1890>
- Medipally, S. R., Yusoff, F. M., Banerjee, S., & Shariff, M. (2015). Microalgae as sustainable renewable energy feedstock for biofuel production. *BioMed Research International*, 2015, 519513. <https://doi.org/10.1155/2015/519513>
- Meeker, D. G., Beenken, K. E., Mills, W. B., Loughran, A. J., Spencer, H. J., Lynn, W. B., & Smeltzer, M. S. (2016). Evaluation of Antibiotics Active against Methicillin-Resistant *Staphylococcus aureus* Based on Activity in an Established Biofilm. *Antimicrobial Agents and Chemotherapy*, 60(10), 5688–5694. <https://doi.org/10.1128/AAC.01251-16>
- Mehra, R., Bhushan, S., Bast, F., & Singh, S. (2019). Marine macroalga *Caulerpa*: role of its metabolites in modulating cancer signaling. *Molecular Biology Reports*, 46(3), 3545–3555. <https://doi.org/10.1007/s11033-019-04743-5>
- Milano, J., Ong, H. C., Masjuki, H. H., Chong, W. T., Lam, M. K., Loh, P. K., & Vellayan, V. (2016). Microalgae biofuels as an alternative to fossil fuel for power generation. *Renewable and Sustainable Energy Reviews*, 58, 180–197. <https://doi.org/10.1016/j.rser.2015.12.150>
- Miller, B. R., & Gulick, A. M. (2016). Structural Biology of Nonribosomal Peptide Synthetases. In B. S. Evans (Ed.), *Nonribosomal Peptide and Polyketide Biosynthesis: Methods and Protocols* (pp. 3–29). Springer New York. [https://doi.org/10.1007/978-1-4939-3375-4\\_1](https://doi.org/10.1007/978-1-4939-3375-4_1)
- Miller, V. L., Taylor, R. K., & Mekalanos, J. J. (1987). Cholera toxin transcriptional activator toxR is a transmembrane DNA binding protein. *Cell*, 48(2), 271–279. [https://doi.org/10.1016/0092-8674\(87\)90430-2](https://doi.org/10.1016/0092-8674(87)90430-2)



- Molina, D., de Carvalho, J. C., Júnior, A. I. M., Faulds, C., Bertrand, E., & Soccol, C. R. (2019). Biological contamination and its chemical control in microalgal mass cultures. *Applied Microbiology and Biotechnology*, 103(23-24), 9345–9358. <https://doi.org/10.1007/s00253-019-10193-7>
- Montefalcone, M., Morri, C., Parravicini, V., & Bianchi, C. N. (2015). A tale of two invaders: divergent spreading kinetics of the alien green algae *Caulerpa taxifolia* and *Caulerpa cylindracea*. *Biological Invasions*, 17(9), 2717–2728. <https://doi.org/10.1007/s10530-015-0908-1>
- Moormeier, D. E., & Bayles, K. W. (2017). *Staphylococcus aureus* biofilm: a complex developmental organism. *Molecular Microbiology*, 104(3), 365–376. <https://doi.org/10.1111/mmi.13634>
- Munro, M. H., Blunt, J. W., Dumdei, E. J., Hickford, S. J., Lill, R. E., Li, S., ... Duckworth, A. R. (1999). The discovery and development of marine compounds with pharmaceutical potential. *Journal of Biotechnology*, 70(1-3), 15–25. [https://doi.org/10.1016/s0168-1656\(99\)00052-8](https://doi.org/10.1016/s0168-1656(99)00052-8)
- Natrah, F. M. I., Kenmegne, M. M., Wiyoto, W., Sorgeloos, P., Bossier, P., & Defoirdt, T. (2011). Effects of micro-algae commonly used in aquaculture on acyl-homoserine lactone quorum sensing. *Aquaculture*, 317(1), 53–57. <https://doi.org/10.1016/j.aquaculture.2011.04.038>
- Newman, D. J., & Cragg, G. M. (2020). Natural Products as Sources of New Drugs over the Nearly Four Decades from 01/1981 to 09/2019. *Journal of Natural Products*, 83(3), 770–803. <https://doi.org/10.1021/acs.jnatprod.9b01285>

Nothias, L.-F., Nothias-Esposito, M., da Silva, R., Wang, M., Protsyuk, I., Zhang, Z., ...

Dorrestein, P. C. (2018). Bioactivity-Based Molecular Networking for the Discovery of Drug Leads in Natural Product Bioassay-Guided Fractionation. *Journal of Natural Products*, 81(4), 758–767. <https://doi.org/10.1021/acs.jnatprod.7b00737>

O'Toole, G., Kaplan, H. B., & Kolter, R. (2000). Biofilm formation as microbial development. *Annual Review of Microbiology*, 54, 49–79. <https://doi.org/10.1146/annurev.micro.54.1.49>

Otto, M. (2018). Staphylococcal Biofilms. *Microbiology Spectrum*, 6(4). <https://doi.org/10.1128/microbiolspec.GPP3-0023-2018>

Pascual, J., Macián, M. C., Arahal, D. R., Garay, E., & Pujalte, M. J. (2010). Multilocus sequence analysis of the central clade of the genus *Vibrio* by using the 16S rRNA, recA, pyrH, rpoD, gyrB, rctB and toxR genes. *International Journal of Systematic and Evolutionary Microbiology*, 60(Pt 1), 154–165. <https://doi.org/10.1099/ij.s.0.010702-0>

Patel, J. B. (2001). 16S rRNA gene sequencing for bacterial pathogen identification in the clinical laboratory. *Molecular Diagnosis: A Journal Devoted to the Understanding of Human Disease through the Clinical Application of Molecular Biology*, 6(4), 313–321. <https://doi.org/10.1054/modi.2001.29158>

Paul, V. J., & Fenical, W. (1986). Chemical defense in tropical green algae, order Caulerpales. *Marine Ecology Progress Series*, 34(1/2), 157–169. <http://www.jstor.org/stable/24824962>

Pawlik, J. R., Amsler, C. D., Ritson-Williams, R., McClintock, J. B., Baker, B. J., & Paul, V. J. (2013). Marine chemical ecology: a science born of scuba. *Research and Discoveries:*

*The Revolution of Science through Scuba*, 53–69.

[https://repository.si.edu/bitstream/handle/10088/21623/SCMS39\\_Lang\\_05.pdf](https://repository.si.edu/bitstream/handle/10088/21623/SCMS39_Lang_05.pdf)

Penesyan, A., Kjelleberg, S., & Egan, S. (2010). Development of novel drugs from marine surface associated microorganisms. *Marine Drugs*, 8(3), 438–459.

<https://doi.org/10.3390/md8030438>

Petersen, L.-E., Kellermann, M. Y., & Schupp, P. J. (2020). Secondary Metabolites of Marine Microbes: From Natural Products Chemistry to Chemical Ecology. In S. Jungblut, V. Liebich, & M. Bode-Dalby (Eds.), *YOUMARES 9 - The Oceans: Our Research, Our Future: Proceedings of the 2018 conference for YOUNg MARine REsearcher in Oldenburg, Germany* (pp. 159–180). Springer International Publishing.

[https://doi.org/10.1007/978-3-030-20389-4\\_8](https://doi.org/10.1007/978-3-030-20389-4_8)

Petras, D., Phelan, V. V., Acharya, D., Allen, A. E., Aron, A. T., Bandeira, N., ... Wang, M. (2022). GNPS Dashboard: collaborative exploration of mass spectrometry data in the web browser. *Nature Methods*, 19(2), 134–136. <https://doi.org/10.1038/s41592-021-01339-5>

Pierucci, A., De La Fuente, G., Cannas, R., & Chiantore, M. (2019). A new record of the invasive seaweed *Caulerpa cylindracea* Sonder in the South Adriatic Sea. *Heliyon*, 5(9), e02449. <https://doi.org/10.1016/j.heliyon.2019.e02449>

Pleil, J. D., & Isaacs, K. K. (2016). High-resolution mass spectrometry: basic principles for using exact mass and mass defect for discovery analysis of organic molecules in blood, breath, urine and environmental media. *Journal of Breath Research*, 10(1), 012001.

<https://doi.org/10.1088/1752-7155/10/1/012001>

- Puglisi, M. P., Sneed, J. M., Sharp, K. H., Ritson-Williams, R., & Paul, V. J. (2014). Marine chemical ecology in benthic environments. *Natural Product Reports*, 31(11), 1510–1553. <https://doi.org/10.1039/c4np00017j>
- Rabin, N., Zheng, Y., Opoku-Temeng, C., Du, Y., Bonsu, E., & Sintim, H. O. (2015). Biofilm formation mechanisms and targets for developing antibiofilm agents. *Future Medicinal Chemistry*, 7(4), 493–512. <https://doi.org/10.4155/fmc.15.6>
- Ramanan, R., Kim, B.-H., Cho, D.-H., Oh, H.-M., & Kim, H.-S. (2016). Algae-bacteria interactions: Evolution, ecology and emerging applications. *Biotechnology Advances*, 34(1), 14–29. <https://doi.org/10.1016/j.biotechadv.2015.12.003>
- Ramón-Peréz, M. L., Diaz-Cedillo, F., Ibarra, J. A., Torales-Cardena, A., Rodríguez-Martínez, S., ... Cancino-Diaz, J. C. (2014). D-Amino acids inhibit biofilm formation in *Staphylococcus epidermidis* strains from ocular infections. *Journal of Medical Microbiology*, 63(Pt 10), 1369–1376. <https://doi.org/10.1099/jmm.0.075796-0>
- Rizzo, L., Frascchetti, S., Alifano, P., Tredici, M. S., & Stabili, L. (2016). Association of *Vibrio* community with the Atlantic Mediterranean invasive alga *Caulerpa cylindracea*. *Journal of Experimental Marine Biology and Ecology*, 475, 129–136. <https://doi.org/10.1016/j.jembe.2015.11.013>
- Robertson, A. W., McCarville, N. G., MacIntyre, L. W., Correa, H., Haltli, B., Marchbank, D. H., & Kerr, R. G. (2018). Isolation of Imaqobactin, an Amphiphilic Siderophore from the Arctic Marine Bacterium *Variovorax* Species RKJM285. *Journal of Natural Products*, 81(4), 858–865. <https://doi.org/10.1021/acs.jnatprod.7b00943>
- Romano, G., Costantini, M., Sansone, C., Lauritano, C., Ruocco, N., & Ianora, A. (2017). Marine microorganisms as a promising and sustainable source of bioactive molecules.

- Marine Environmental Research*, 128, 58–69.  
<https://doi.org/10.1016/j.marenvres.2016.05.002>
- Roy, R., Tiwari, M., Donelli, G., & Tiwari, V. (2018). Strategies for combating bacterial biofilms: A focus on anti-biofilm agents and their mechanisms of action. *Virulence*, 9(1), 522–554. <https://doi.org/10.1080/21505594.2017.1313372>
- Rushdi, M. I., Abdel-Rahman, I. A. M., Attia, E. Z., Abdelraheem, W. M., Saber, H., Madkour, H. A., ... Abdelmohsen, U. R. (2020). A review on the diversity, chemical and pharmacological potential of the green algae genus *Caulerpa*. *South African Journal of Botany*, 132, 226–241. <https://doi.org/10.1016/j.sajb.2020.04.031>
- Russo, P., Nastrucci, C., & Cesario, A. (2011). From the sea to anticancer therapy. *Current Medicinal Chemistry*, 18(23), 3551–3562. <https://doi.org/10.2174/092986711796642652>
- Saitou, N., & Nei, M. (1987). The neighbor-joining method: a new method for reconstructing phylogenetic trees. *Molecular Biology and Evolution*, 4(4), 406–425.  
<https://doi.org/10.1093/oxfordjournals.molbev.a040454>
- Salaün, S., La Barre, S., Dos Santos-Goncalvez, M., Potin, P., Haras, D., & Bazire, A. (2012). Influence of exudates of the kelp *Laminaria digitata* on biofilm formation of associated and exogenous bacterial epiphytes. *Microbial Ecology*, 64(2), 359–369.  
<https://doi.org/10.1007/s00248-012-0048-4>
- Sanger, F., Nicklen, S., & Coulson, A. R. (1977). DNA sequencing with chain-terminating inhibitors. *Proceedings of the National Academy of Sciences of the United States of America*, 74(12), 5463–5467. <https://doi.org/10.1073/pnas.74.12.5463>

- Santos, J. D., Vitorino, I., Reyes, F., Vicente, F., & Lage, O. M. (2020). From Ocean to Medicine: Pharmaceutical Applications of Metabolites from Marine Bacteria. *Antibiotics (Basel, Switzerland)*, 9(8). <https://doi.org/10.3390/antibiotics9080455>
- Sarker, S. D., Latif, Z., & Gray, A. I. (2005). Natural Product Isolation. In S. D. Sarker, Z. Latif, & A. I. Gray (Eds.), *Natural Products Isolation* (pp. 1–25). Humana Press. <https://doi.org/10.1385/1-59259-955-9:1>
- Satola, B., Wübbeler, J. H., & Steinbüchel, A. (2013). Metabolic characteristics of the species *Variovorax paradoxus*. *Applied Microbiology and Biotechnology*, 97(2), 541–560. <https://doi.org/10.1007/s00253-012-4585-z>
- Scherlach, K., & Hertweck, C. (2021). Mining and unearthing hidden biosynthetic potential. *Nature Communications*, 12(1), 3864. <https://doi.org/10.1038/s41467-021-24133-5>
- Schilcher Katrin, & Horswill Alexander R. (2020). Staphylococcal Biofilm Development: Structure, Regulation, and Treatment Strategies. *Microbiology and Molecular Biology Reviews: MMBR*, 84(3), e00026–19. <https://doi.org/10.1128/MMBR.00026-19>
- Schmidt, R., Ulanova, D., Wick, L. Y., Bode, H. B., & Garbeva, P. (2019). Microbe-driven chemical ecology: past, present and future. *The ISME Journal*, 13(11), 2656–2663. <https://doi.org/10.1038/s41396-019-0469-x>
- Shao, W., Khin, S., & Kopp, W. C. (2012). Characterization of effect of repeated freeze and thaw cycles on stability of genomic DNA using pulsed field gel electrophoresis. *Biopreservation and Biobanking*, 10(1), 4–11. <https://doi.org/10.1089/bio.2011.0016>
- Sharma, D., Misba, L., & Khan, A. U. (2019). Antibiotics versus biofilm: an emerging battleground in microbial communities. *Antimicrobial Resistance and Infection Control*, 8, 76. <https://doi.org/10.1186/s13756-019-0533-3>

- Sheahan, M., Gould, C. A., Neumann, J. E., Kinney, P. L., Hoffmann, S., Fant, C., ... Kolian, M. (2022). Examining the Relationship between Climate Change and Vibriosis in the United States: Projected Health and Economic Impacts for the 21st Century. *Environmental Health Perspectives*, 130(8), 87007. <https://doi.org/10.1289/EHP9999a>
- Silvester, R., Alexander, D., Antony, A. C., & Hatha, M. (2017). GroEL PCR- RFLP - An efficient tool to discriminate closely related pathogenic *Vibrio* species. *Microbial Pathogenesis*, 105, 196–200. <https://doi.org/10.1016/j.micpath.2017.02.029>
- Sleno, L. (2012). The use of mass defect in modern mass spectrometry. *Journal of Mass Spectrometry: JMS*, 47(2), 226–236. <https://doi.org/10.1002/jms.2953>
- Sneed, J. M., & Pohnert, G. (2011). The green alga *Dicytosphaeria ocellata* and its organic extracts alter natural bacterial biofilm communities. *Biofouling*, 27(4), 347–356. <https://doi.org/10.1080/08927014.2011.576317>
- Steinberg, P. D., De Nys, R., & Kjelleberg, S. (2002). Chemical cues for surface colonization. *Journal of Chemical Ecology*, 28(10), 1935–1951. <https://doi.org/10.1023/a:1020789625989>
- Stocker, R., & Seymour, J. R. (2012). Ecology and physics of bacterial chemotaxis in the ocean. *Microbiology and Molecular Biology Reviews: MMBR*, 76(4), 792–812. <https://doi.org/10.1128/MMBR.00029-12>
- Thompson, F. L., Gevers, D., Thompson, C. C., Dawyndt, P., Naser, S., Hoste, B., ... Swings, J. (2005). Phylogeny and molecular identification of vibrios on the basis of multilocus sequence analysis. *Applied and Environmental Microbiology*, 71(9), 5107–5115. <https://doi.org/10.1128/AEM.71.9.5107-5115.2005>

- Thompson, F. L., Iida, T., & Swings, J. (2004). Biodiversity of vibrios. *Microbiology and Molecular Biology Reviews: MMBR*, 68(3), 403–431.  
<https://doi.org/10.1128/MMBR.68.3.403-431.2004>
- Throck Watson, J., & David Sparkman, O. (2007). *Introduction to Mass Spectrometry: Instrumentation, Applications, and Strategies for Data Interpretation* (4th ed.). John Wiley & Sons.
- Tolker-Nielsen, T. (2015). Biofilm Development. *Microbiology Spectrum*, 3(2), MB – 0001–2014. <https://doi.org/10.1128/microbiolspec.MB-0001-2014>
- Trivella, D. B. B., & de Felicio, R. (2018). The Tripod for Bacterial Natural Product Discovery: Genome Mining, Silent Pathway Induction, and Mass Spectrometry-Based Molecular Networking. *mSystems*, 3(2). <https://doi.org/10.1128/mSystems.00160-17>
- U.S. National Library of Medicine. (n.d.). *BLAST Frequently Asked Questions*. National Center for Biotechnology Information. Retrieved August 25, 2022, from [https://blast.ncbi.nlm.nih.gov/Blast.cgi?CMD=Web&PAGE\\_TYPE=BlastDocs&DOC\\_TYPE=FAQ](https://blast.ncbi.nlm.nih.gov/Blast.cgi?CMD=Web&PAGE_TYPE=BlastDocs&DOC_TYPE=FAQ)
- Udworthy, D. W., Zeigler, L., Asolkar, R. N., Singan, V., Lapidus, A., Fenical, W., ... Moore, B. S. (2007). Genome sequencing reveals complex secondary metabolome in the marine actinomycete *Salinispora tropica*. *Proceedings of the National Academy of Sciences of the United States of America*, 104(25), 10376–10381.  
<https://doi.org/10.1073/pnas.0700962104>
- Van de Peer, Y., Chapelle, S., & De Wachter, R. (1996). A quantitative map of nucleotide substitution rates in bacterial rRNA. *Nucleic Acids Research*, 24(17), 3381–3391.  
<https://doi.org/10.1093/nar/24.17.3381>



- Vezzulli, L., Colwell, R. R., & Pruzzo, C. (2013). Ocean warming and spread of pathogenic vibrios in the aquatic environment. *Microbial Ecology*, 65(4), 817–825.  
<https://doi.org/10.1007/s00248-012-0163-2>
- Walters, L. J., Brown, K. R., Stam, W. T., & Olsen, J. L. (2006). E-commerce and Caulerpa: unregulated dispersal of invasive species. *Frontiers in Ecology and the Environment*, 4(2), 75–79. [https://doi.org/10.1890/1540-9295\(2006\)004\[0075:eacudo\]2.0.co;2](https://doi.org/10.1890/1540-9295(2006)004[0075:eacudo]2.0.co;2)
- Wang, B., Lan, C. Q., & Horsman, M. (2012). Closed photobioreactors for production of microalgal biomasses. *Biotechnology Advances*, 30(4), 904–912.  
<https://doi.org/10.1016/j.biotechadv.2012.01.019>
- Wang, B., Li, Y., Wu, N., & Lan, C. Q. (2008). CO<sub>2</sub> bio-mitigation using microalgae. *Applied Microbiology and Biotechnology*, 79(5), 707–718. <https://doi.org/10.1007/s00253-008-1518-y>
- Wang, H., Hill, R. T., Zheng, T., Hu, X., & Wang, B. (2014). Effects of bacterial communities on biofuel-producing microalgae: stimulation, inhibition and harvesting. *Critical Reviews in Biotechnology*, 36(2), 341–352. <https://doi.org/10.3109/07388551.2014.961402>
- Weisburg, W. G., Barns, S. M., Pelletier, D. A., & Lane, D. J. (1991). 16S ribosomal DNA amplification for phylogenetic study. *Journal of Bacteriology*, 173(2), 697–703.  
<https://doi.org/10.1128/jb.173.2.697-703.1991>
- Wolfender, J.-L., Nuzillard, J.-M., van der Hooft, J. J. J., Renault, J.-H., & Bertrand, S. (2019). Accelerating Metabolite Identification in Natural Product Research: Toward an Ideal Combination of Liquid Chromatography-High-Resolution Tandem Mass Spectrometry and NMR Profiling, in Silico Databases, and Chemometrics. *Analytical Chemistry*, 91(1), 704–742. <https://doi.org/10.1021/acs.analchem.8b05112>

- Xu, R., Ye, Y., & Zhao, W. (2011). *Introduction to Natural Products Chemistry*. CRC Press.
- Yan, Z., Huang, M., Melander, C., & Kjellerup, B. V. (2020). Dispersal and inhibition of biofilms associated with infections. *Journal of Applied Microbiology*, 128(5), 1279–1288. <https://doi.org/10.1111/jam.14491>
- Yang, L., Liu, Y., Wu, H., Song, Z., Høiby, N., Molin, S., & Givskov, M. (2012). Combating biofilms. *FEMS Immunology and Medical Microbiology*, 65(2), 146–157. <https://doi.org/10.1111/j.1574-695X.2011.00858.x>
- Yao, S., Lyu, S., An, Y., Lu, J., Gjermansen, C., & Schramm, A. (2019). Microalgae-bacteria symbiosis in microalgal growth and biofuel production: a review. *Journal of Applied Microbiology*, 126(2), 359–368. <https://doi.org/10.1111/jam.14095>
- Zhu, Z., Jiang, J., & Fa, Y. (2020). Overcoming the Biological Contamination in Microalgae and Cyanobacteria Mass Cultivations for Photosynthetic Biofuel Production. *Molecules* , 25(22), 5220. <https://doi.org/10.3390/molecules25225220>
- Ziemert, N., Alanjary, M., & Weber, T. (2016). The evolution of genome mining in microbes - a review. *Natural Product Reports*, 33(8), 988–1005. <https://doi.org/10.1039/c6np00025h>
- Zittelli, G. C., Biondi, N., Rodolfi, L., & Tredici, M. R. (2013). Photobioreactors for Mass Production of Microalgae. In *Handbook of Microalgal Culture* (pp. 225–266). John Wiley & Sons, Ltd. <https://doi.org/10.1002/9781118567166.ch13>